ACTA MEDICA MARTINIANA

PATHOPHYSIOLOGY OF AIRWAY AFFERENT NERVES

JAKUSOVA JANKA, PECOVA RENATA

Department of Pathological Physiology, Jessenius Faculty of Medicine in Martin, Comenius University of Bratislava, Martin, Slovak Republic

A b s t r a c t

Vagal afferent nerves provide an airway defense mechanism which is ensured by their activation. These nerves can be activated mechanically mainly through mechanosensitive Aβ fibers which are divided into slowly adapting (SARs) and rapidly adapting stretch receptors (RARs). Chemical activation is provided by an interaction of chemical substances with specific receptors. C-fibers are highly sensitive to a direct chemical stimulation accomplished by an activation of ligand-gated ion channels. According to the large influence and mechanisms of vagal afferent nerves, there is a probability that an inappropriate activity of these nerves can cause the symptoms of the respiratory diseases, e.g. cough, dyspnoea, or airway hyperreactivity. The aim of this review is to summarize the physiology of airway afferent nerves and point out the role of vagal sensory nerves dysfunction in the pathogenesis of some respiratory diseases. The understanding of its mechanism could lead to new therapeutic strategies in patients with airway-related pathology.

Keywords: A-fibers · C-fibers · Vagal nerves · Cough receptors

INTRODUCTION

Due to the high incidence of respiratory diseases it is important to know the role of afferent nerve endings in the pathogenesis of these diseases. This review article provides an overview of afferent nerve endings in the airways and their involvement in disease pathogenesis. The main function of vagal afferent nerves is to provide a defense mechanism which leads to an unpolluted environment. Cough is the main defensive airway reflex and can be triggered by various stimuli to the mainly laryngeal and tracheobronchial cough receptors. However, these receptors can also be scattered in the diaphragm, pleura, or oesophagus. Information from the receptors passes along afferent nerves to the complex neuronal cough network in the brainstem where it is processed. The output information from the cough network targets the effector muscles eliciting the cough reflex (1). The activation of some afferent nerves can cause either urge to cough, coughing, or sensations of dyspnoea. This mechanism can also become dysregulated in disorders that involve inflammation, such as bronchial asthma, rhinitis, bronchitis, or chronic obstructive pulmonary disease. Patients may also suffer from an excessive sneezing, coughing, dyspnoea, eventually bronchospasm, and secretion as parts of the autonomic reflexes (2).

Corresponding author: Janka Jakusova, MD.; e-mail: jakusova20@uniba.sk

CLASSIFYING AIRWAY AFFERENT NERVES

A. Characterisation of Anatomical/Morphological Properties
Airway environment is monitored by sensory neural innervation with afferent sensors which supplies the respiratory tree. This innervation is derived from multiple sources including several cranial and spinal nerves. The nasal passages are innervated by the trigeminal ganglia with sensory fibers that reach the nasal mucosa through the anterior ethmoidal nerve. At the lower part of the airways, trigeminal innervation is replaced by vagal and glossopharyngeal innervation, especially in the nasopharynx, pharynx, and soft palate. Larynx and lower airways are supplied mostly by vagal innervation, where the branches of the vagus nerve (the pharyngeal, superior laryngeal, recurrent laryngeal, and pulmonary branches) are involved. The vagal afferents are derived from the jugular or nodose ganglia, but the glossopharyngeal afferents have their soma in the petrosal ganglion (Table I). In some animal species there is a semi-fused or completely fused single ganglion complex composed of these three ganglia. Nodose and jugular neurons are preferentially located in the rostral and caudal poles of the ganglion complex (2).

B. Characterisation Based on Fiber Conduction Velocities
The type and diameter of the nerves and the degree of their myelination mostly affect the velocity of action potentials passing down the axon. The action potential can be triggered by mechanical, electrical, or chemical stimulation. In the vagus nerve the sensory compound potential consists of the fastest Aβ fibers, intermediate Aδ fibers, and the slowest C-fibers (2). Studies of Undem et al. (3) from 2004 subclassified vagal C-fibers as jugular or nodose depending on where the cell body is located. The cell body can be situated in the nodose (placodal-derived) or jugular (neural crest-derived) ganglia. Studies in guinea pigs and mice showed the differences between jugular and nodose C-fibers. The nodose C-fibers are stimulated by more chemical stimuli than jugular C-fibers, but these can contain more sensory neuropeptides than nodose C-fibers (3). Both of these C-fibers can respond to potentially damaging mechanical forces, inflammatory mediators, and tissue acidification (4). On the other hand, the A-fibers are derived from nodose neurons and they respond to mechanical forces with low thresholds (Table I). There are Aδ-fibers and Aβ-fibers. The Aδ-fibers are also known as cough receptors. These fibers have been described in guinea pigs in the extrapulmonary bronchi, trachea, and larynx (5). However, nerves with similar structures as Aδ-fibers were described also in human bronchi (6). In comparison, Aδ-fibers are very sensitive to mechanical stimulation of the epithelium, but their response to tissue distension, inflammatory mediators, and muscle contraction is lower. Also, these fibers are sensitive to acid, but only when there is a significant decrease in pH (7). The Aβ-fibers are subcategorised as slowly adapting receptors known as SARs or rapidly adapting receptors known as RARs. This classification is based on the adaptation of their firing activity during long-term stimulation. Aβ-fibers are sensitive to lung deflation caused by mechanical forces (8) and also to the lung distention which was evoked by inspiration (2). According to Kaufman et al. (9), SARs are also more sensitive to lung inflation than RARs. This study has shown that SARs respond to transpulmonary pressures of ~ 6 cmH$_2$O, but RARs required pressures of about 13 cmH$_2$O.

C. Characterisation Based on Physiological Responsiveness
The anatomical distribution of SARs and RARs in the airway wall has not been well described. According to functional studies, RARs are located in the intrapulmonary and extrapulmonary airways and terminate within or beneath the epithelium, while SARs are associated with the smooth muscle of the airways. The most important feature of RARs is their rapid adaptation to sustained lung inflations, which is approximately 1-2 seconds. On the other hand, SARs differ from RARs by airway distribution and their action

potential conduction velocities. SARs are slowly adapting stretch receptors which are (similar to RARs) highly sensitive to mechanical forces in the lungs during respiratory cycles. Obstruction or bronchospasm can secondarily lead to an increased activity of the pulmonary mechanoreceptors. RARs or SARs can be activated by a wide variety of endogenous and exogenous substances, such as acetylcholine, histamine, capsaicin, bradykinin, or substance P. This activation results in an inhibition of the local end organ effects. RARs are also known as irritant receptors, however, this term is misleading due to their role in the control of breathing, and by finding that only a few chemical stimuli can activate RAR or SAR intrapulmonary mechanoreceptor (2). Cough receptors are distinct from RARs and SARs due to their low tendency to be activated by tissue stretch but they promptly respond to punctate mechanical stimuli. They are also highly responsive to changes in luminal pH and hypotonic solutions which depend on the expression of Ca^{2+} activated chloride channels and acid sensing ion channels (7). In addition, cough receptors are unresponsive to airway distension and to many chemical stimuli and bronchospastic agents (indirectly activating other pulmonary mechanosensors). Compared to RARs and SARs, the cough receptor afferents are myelinated, however, their conduction velocity is lower than intrapulmonary RARs and SARs. Cough receptors are low threshold mechanoreceptors derived from nodose ganglia which are placed within the large airways, as well. In guinea pigs, these receptors represent the only significant population of nodose-derived A- fibers in the large airways. The guinea pig trachea contains approx. 180 cough receptors afferent terminals and the vagus nerve in the tracheal wall contains equal number of receptors ipsilaterally (5). Studies have shown that afferent terminals are derived from nodose ganglia and correspond to touch sensitive fibers which mediate mechanically evoked cough. On the other hand, chemically sensitive afferents can be non-myelinated (C-type) or lightly myelinated (Aδ-type) fibers. These afferents are especially sensitive to capsaicin, a pungent component of chili peppers, with the expression of the capsaicin-sensitive ion channel TRPV1 (10). Non-myelinated afferent C-fibers are different from mechanosensitive afferents by their direct responsiveness to chemical substances at ligand-gated ion channels and their conduction velocity (4). Endings of C-fibers are polymodal, so they can respond to chemical and mechanical stimulation. Generally, C-fibers do not fire action potentials due to their high threshold for mechanical activation but rather react to noxious chemicals, during tissue injury, or to inflammation. In addition, proinflammatory mediators can sensitise C-fibers and lower their threshold for activation by various stimuli, e.g. bronchoconstriction may activate C-fibers in the diseased airways (11).

Table 1. Vagal sensory neurons mediating cough (12)

Neuron type	Mechanoreceptor A-fibers	Nociceptor A and C-fibers
Vagal origin	Nodose ganglia	Jugular ganglia
Terminations	Larynx Trachea Main bronchi	Broadly throughout airways and lungs
Stimuli	Touch/punctate Acidic solutions Low Cl− solutions	Wide range of chemicals and inflammatory mediators

MECHANISMS IN ACTIVATION OF AIRWAY AFFERENT NERVES

A. Mechanical Activation

The respiratory tract is supplied by sensory nerves which can be all stimulated to evoke action potentials by a mechanical stimulation of the nerve terminals. The nodose and jugular C-fibers are classified as high-threshold mechanosensors, except for certain pulmonary C-fibers which are reffered to as weakly responding to a lung distension during inspiration. However, Aβ-fibers are very sensitive to a lung distention caused by deep inspiration or even in eupneic breathing. Generally considered, SAR fibers respond to increases in circumferential tension on the wall of trachea, the rate of distension, and the changes of transpulmonary pressure (2). RAR fibers also respond to increases in transpulmonary pressure. The increase of transpulmonary pressure results in a rise of number of action potential discharge at a constant rate of inflation (13). In contrast, RAR fibers are sensitive to changes in lung compliance unlike SARs. Decrease in lung compliance causes RAR fibers to be more sensitive to mechanical activation (2).

B. Chemical Activation

There are not only mechanosensitive vagal afferent nerves in the respiratory tract but also chemosensitive nerves that communicate with the CNS about the chemical environment in which they terminate. A wide range of chemicals can interact with specific receptors and then evoke action potential discharge. A direct chemical activation of afferent nerve terminals is accomplished by an activation of ligand-gated ion channels. These are nonspecific cation channels. The ligand binds to these receptors with high selectivity and sensitivity, leading to a signaling cascade at the afferent nerve terminals that closes or opens channels and then causes a depolarizing generator potential (2). A large family of ion channels composes transient receptor potential channel (TRP). TRPV1 receptor was also known as the vanilloid receptor, because the vanilloid moiety on capsaicin and potential capsaicin analog named resiniferatoxin selectively bind to this receptor. Capsaicin activates most of the afferent C-fibers innervating the respiratory tract irrespective of their ganglionic origin or terminal location. However, in mice, a significant percentage of afferent C-fibers is capsaicin-insensitive (14). The activation of generally all C-fibers in the respiratory tract can be caused by an acidic environment. In the guinea pig trachea, the acid induced action potential discharge in jugular C-fibers is partially inhibited by TRPV1 blocking drugs, and in capsaicin sensitive C-fibers in the mouse lungs these were largely inhibited, too (7,14). The acidic environment can also activate A-fibers in the respiratory tract, especially the nodose Aδ cough receptors in the guinea pig trachea are more sensitive to acid than the tracheal C-fibers. These do not express TRPV1 and the acid induced action potential discharge is not inhibited by TRPV1 blockers (7). Further studies have shown that TRPV1 receptor is also heat and acid sensitive. In the presence of acidic conditions, the amount of heat needed to activate the channel is reduced and vice versa (15). A temperature needed to activate TRPV1 is approximately 43 °C, which is difficult to reach in a healthy respiratory tract (16). On the other hand, hyperthermic temperatures may increase the sensitivity of the channel to other stimuli that can affect the respiratory tract (17).

EVIDENCE OF VAGAL SENSORY NERVE DYSFUNCTION IN AIRWAY DISEASE

Alterations in the nervous system often cause the symptoms of the respiratory diseases, e.g. urge to cough, coughing, excessive sneezing, reflex bronchospasm, mucus secretions, sensations of dyspnea, or painful oropharynx. There is a probability that an inappropriate activity within the afferent nervous system can cause all these symptoms (2). Chronic nasal

symptoms attributable to a sensory nerve activation in patients with rhinitis implicate that the inflammation leads to a repeated activation of sensory nerves. The repeated activation and mediators associated with inflammation can induce sensitisation at multiple levels of sensory pathways. Thus, we predicted that the cough reflex is more sensitive in patients with allergic rhinitis than in healthy subjects. During the allergic atopic process, the functional change of airway afferent nerve-endings mediating cough response can be shown by capsaicin cough test (18,19,20).

A. Wheezing and Airway Hyperreactivity

The parasympathetic nervous system is likely the dominant regulator of bronchial smooth muscle tone and provides cholinergic contractile innervation and VIP/nitrergic relaxant innervation to the smooth muscles. In the respiratory tract, the parasympathetic contractile reflex can be increased by an activation of RAR fibers and vagal C-fibers. During an asthma attack there can be wheezing caused precisely because of contractions of bronchial smooth muscle, which lead to an airway narrowing (21). According to studies with asthmatic subjects, enlarging the airways and decreasing the resistance to airflow can be induced by blocking cholinergic contractile activity (22,23). Bronchial hyperreactivity is a hallmark of asthma, but some studies support the idea that it can be actually a hyperreflexivity. Hyperreactivity is identified by the concentrations of a bronchoconstrictor stimulants, e.g. methacholine or histamine, required to increase the airway resistance by 20% (2). However, studies in mice have shown that inhaling this stimulant in asthmatic subjects can evoke a strong parasympathetic reflex, which is not seen in healthy volunteers (24).

B. Dyspnoea

Dyspnoea can be described as sensations of air hunger and chest tightness. Dyspnoeic sensations in some individuals can be caused by electrical stimulation of the cervical vagal nerves (25). The sensations of dyspnoea can also be evoked with exercise and by inhalation of mediators, e.g. histamine, adenosine, and prostaglandin E2 that can activate vagal afferent nerves and intensify dyspnoea (26, 27).

C. Chronic Cough

In the past, chronic cough was assumed to occur because of various primary disorders, such as asthma, postnasal drip syndrome, or gastroesophageal reflux disease. Today, there is a presumption of cough as a primary disorder which has similarities with chronic pain syndromes (2). In chronic pain there are allodynia and hyperalgesia, whereas in chronic cough there are conditions called hypertussivity and allotussivity. Hypertussivity is an excessive response to the tussive stimulus (most often to inhaled capsaicin), but in allotussivity the strong urge to cough is induced by nontussive stimuli, such as singing, laughing, and talking (28).

D. The Urge to Cough

The urge to cough is referred to as an interoceptive experience informing the brain of the internal environment of the pulmonary system. However, the urge to cough is difficult to study, as well as dyspnoea, due to a psychophysical nature of the sensations. Recent studies with adult volunteers have shown that in patients with a respiratory disease the stimulus threshold for evoking an urge to cough is significantly reduced, but in patients with chronic cough there is an ongoing perception of an urge to cough, which is not experienced by healthy people. According to these studies there is a presumption of disease-induced sensory hypersensitivity and enhanced basal vagal afferent activity (29, 30).

CONCLUSION

Very little is known about vagal sensory processing in humans, which does not allow a valid comparison between animal and human systems. Knowledge of the morphology and function of afferent nerve endings in the airways is important for understanding the pathogenesis of many respiratory diseases. Future research in this area should focus on new therapeutic goals and strategies aimed at those suffering from airway-related pathology. Monitoring activity of afferent nerve endings in the airways with a capsaicin test can help with objectivisation of cough as the most common symptom of respiratory diseases. A single-breath method of capsaicin aerosol inhalation is the most widespread technique in the assessment of cough reflex sensitivity (30). Dysregulation of the vagal sensory neurons mediating cough is thought to give rise to chronic cough. According to a study from 2021 (31), several molecular targets have been investigated in the pathophysiology of refractory chronic cough and unexplained chronic cough. Although there are currently no new approved treatments for these conditions and data have varied between investigative approaches, promising results have been reported. Further multidisciplinary research is needed to establish the best treatment pathways for patients with airway-related pathology due to heterogeneity of chronic cough.

REFERENCES

1. Korpáš J, Tomori Z. Cough and other respiratory reflexes. In: Herzog H, editor. Basel: Karger, 1979; 1-356.
2. Mazzone SB, Undem BJ. Vagal Afferent Innervation of the Airways in Health and Disease. Physiol Rev.2016; 96(3): 975-1024.
3. Undem BJ, Chuaychoo B, Lee MG, Weinreich D, Myers AC, Kollarik M. Subtypes of vagal afferent C fibers in guinea pig lungs. J Physiol 2004; 556: 905–917.
4. Ho CY, Gu Q, Lin YS, Lee LY. Sensitivity of vagal afferent endings to chemical irritants in the rat lung. Respir Physiol 2001; 127: 113–124.
5. Canning BJ, Mazzone SB, Meeker SN, Mori N, Reynolds SM, Undem BJ. Identification of the tracheal and laryngeal afferent neurones mediating cough in anaesthetized guinea-pigs. J Physiol 2004; 557: 543–558.
6. West PW, Canning BJ, Merlo-Pich E, Woodcock AA, Smith JA. Morphologic characterization of nerves in whole-mount airway biopsies. Am J Respir Crit Care Med 2015; 192: 30–39.
7. Kollarik M, Undem BJ. Mechanisms of acid-induced activation of airway afferent nerve fibres in guinea-pig. J Physiol 2002; 543: 591–600.
8. Liu J, Yu J. Spectrum of myelinated pulmonary afferents (II). Am J Physiol Regul Integr Comp Physiol 2013; 305: R1059–R1064.
9. Kaufman MP, Iwamoto GA, Ashton JH, Cassidy SS. Responses to inflation of vagal afferents with endings in the lung of dogs. Circ Res 1982; 51: 525–531.
10. Lin YJ, Lin RL, Ruan T, Khosravi M, Lee LY. A synergistic effect of simultaneous TRPA1 and TRPV1 activations on vagal pulmonary C-fiber afferents. J Appl Physiol 2015; 118: 273–281.
11. Wang AL, Blackford TL, Lee LY. Vagal bronchopulmonary C-fibers and acute ventilatory response to inhaled irritants. Respir Physiol 1996; 104: 231–239.
12. McGovern AE, Short KR, Moe AAK, Mazzone SB. Translational review: Neuroimmune mechanisms in cough and emerging therapeutic targets. Journal of Allergy and Clinical Immunology 2018; 142 (5): 1392-1402.
13. Pack AI, DeLaney RG. Response of pulmonary rapidly adapting receptors during lung inflation. J Appl Physiol 1983; 55: 955–963.
14. Kollarik M, Dinh QT, Fischer A, Undem BJ. Capsaicin-sensitive and insensitive vagal bronchopulmonary C-fibres in the mouse. J Physiol 2003; 551: 869–879.

15. Tominaga M, Caterina MJ, Malmberg AB, Rosen TA, Gilbert H, Skinner K, Raumann BE, Basbaum AI, Julius D. The cloned capsaicin receptor integrates multiple pain-producing stimuli. Neuron 1998; 21: 531–543.
16. Ni D, Gu Q, Hu HZ, Gao N, Zhu MX, Lee LY. Thermal sensitivity of isolated vagal pulmonary sensory neurons: role of transient receptor potential vanilloid receptors. Am J Physiol Regul Integr Comp Physiol 2006; 291: R541–R550.
17. Voets T, Droogmans G, Wissenbach U, Janssens A, Flockerzi V, Nilius B. The principle of temperature-dependent gating in cold- and heat-sensitive TRP channels. Nature 2004; 430: 748–754.
18. Pecova R, Frlickova Z, Pec J, Tatar M. Cough sensitivity in atopic dermatitis. Pulm Pharmacol Ther 2003, 16(4): 203-206.
19. Pecova R, Vrlik M, Tatar M. Cough sensitivity in allergic rhinitis. J Physiol Pharmacol. 2005; 56 (Suppl. 4): 171-178.
20. Pecova R, Zucha J, Pec M, Neuschlova M, Hanzel P, Tatar M. Cough reflex sensitivity testing in seasonal allergic rhinitis patients and healthy volunteers. J Physiol Pharmacol. 2008; 59 (Suppl 6): 557-64.
21. Undem BJ, Potenzieri C. Autonomic neural control of intrathoracic airways. Comp Physiol 2012; 2: 1241–1267.
22. Grandordy BM, Thomas V, de Lauture D, Marsac J. Cumulative dose-response curves for assessing combined effects of salbutamol and ipratropium bromide in chronic asthma. Eur Respir J 1988; 1: 531–535.
23. Gross NJ, Skorodin MS. Anticholinergic, antimuscarinic bronchodilators. Am Rev Respir Dis 1984; 129: 856–870.
24. McAlexander MA, Gavett SH, Kollarik M, Undem BJ. Vagotomy reverses established allergen-induced airway hyperreactivity to methacholine in the mouse. Respir Physiol Neurobiol 2015; 212–214: 20–24.
25. Handforth A, DeGiorgio CM, Schachter SC, Uthman BM, Naritoku DK, Tecoma ES, Henry TR, Collins SD, Vaughn BV, Gilmartin RC, Labar DR, Morris GL 3rd, Salinsky MC, Osorio I, Ristanovic RK, Labiner DM, Jones JC, Murphy JV, Ney GC, Wheless JW. Vagus nerve stimulation therapy for partial-onset seizures: a randomized active-control trial. Neurology 1998; 51: 48–55.
26. Taguchi O, Kikuchi Y, Hida W, Iwase N, Okabe S, Chonan T, Takishima T. Prostaglandin E2 inhalation increases the sensation of dyspnea during exercise. Am Rev Respir Dis 1992; 145: 1346–1349.
27. Tetzlaff K, Leplow B, ten Thoren C, Dahme B. Perception of dyspnea during histamine- and methacholine-induced bronchoconstriction. Respiration 1999; 66: 427–433.
28. Hilton E, Marsden P, Thurston A, Kennedy S, Decalmer S, Smith JA. Clinical features of the urge-to-cough in patients with chronic cough. Respir Med 2015; 109: 701–707.
29. Dicpinigaitis PV, Bhat R, Rhoton WA, Tibb AS, Negassa A. Effect of viral upper respiratory tract infection on the urge-to-cough sensation. Respir Med 2011; 105: 615–618.
30. Morice AH, Millqvist E, Bieksiene K, Birring SS, Dicpinigaitis P, Domingo Ribas C, Hilton Boon M, Kantar A, Lai K, McGarvey L, Rigau D, Satia I, Smith J, Song WJ, Tonia T, van den Berg JWK, van Manen MJG, Zacharasiewicz A. ERS guidelines on the diagnosis and treatment of chronic cough in adults and children. Eur Respir J. 2020; 55(1).
31. Mazzone SB, McGarvey L. Mechanisms and Rationale for Targeted Therapies in Refractory and Unexplained Chronic Cough. Clin Pharmacol Ther. 2021; 109(3): 619–636.

COMPUTER MODELING OF D, L – HOMOCYSTEIC ACID MICROINJECTION INTO THE BÖTZINGER COMPLEX AREA

VETERNIK MARCEL[1], MARTVON LUKAS[2], MISEK JAKUB[1], SIMERA MICHAL[1], POLIACEK IVAN[1]

[1] Department of Medical Biophysics, Jessenius Faculty of Medicine in Martin, Comenius University in Bratislava, Slovak Republic
[2] Medical Education Support Center, Jessenius Faculty of Medicine in Martin, Comenius University in Bratislava, Slovak Republic

Abstract

The impact of D,L – homocysteic acid (DLH) microinjection (non-specific glutamate receptor agonist that causes excitation of neurons) into the Bötzinger complex area (BOT) was simulated using computer model of quiet breathing and cough reflex. Integrated signals from simulated neuronal populations innervating inspiratory phrenic and expiratory lumbar motoneurons were obtained. We analysed durations and amplitudes of these "pre-phrenic and pre-lumbar" activities during quiet breathing and cough reflex and the number of coughs elicited by a fictive 10-second-long stimulation. Model fibre population provides virtual DLH related excitation to expiratory neuronal populations with augmenting discharge pattern (BOT neurons). The excitation was modelled by a higher number of fibres and terminals (simulated a higher number of excitatory inputs) or by a higher synaptic strength (simulated a higher effect of excitatory inputs).

Our simulations have demonstrated a high analogy of cough and breathing changes to those observed in animal experiments. The simulated neuronal excitations in the BOT led to cough depression represented by a lower cough number and a cough neuronal activity of the lumbar nerve. Despite the shortening of the phrenic activity during cough (compared to quiet breathing), which was not observed in animal experiments, our simulations confirm the ability of the computer model to simulate motor processes in the respiratory system. The computer model of functional respiratory / cough neural network is capable to confirm and / or predict the results obtained on animals.

Keywords: cough, breathing, simulation, modulation, excitation, neuron

INTRODUCTION

The Bötzinger complex is a neuronal population of expiratory (E) neurons with augmenting (AUG) discharge pattern. It is located in the rostral part of the ventral respiratory column (VRC) near the retrofacial nucleus (1, 2, 3). Some expiratory units with decrementing (DEC) discharge patterns (4), as well as other respiratory related neurons are found in the BOT and surrounding reticular formation (5, 6). The BOT region and the pre-Bötzinger complex (pre-BOT) are important in generation of respiratory rhythm and modulation of expiratory motor activity (2, 7) resulting in shaping and timing of inspiratory and expiratory phases (2, 8). BOT E-AUG and E-DEC neurons have many axonal connections with respiratory neurons in other brainstem areas. Most of the BOT E units inhibit inspiratory as well as expiratory neurons in the VRC, dorsal respiratory group, and also phrenic motoneurons (1, 3).

The respiratory neuronal network in BOT / pre-BOT significantly participate in the generation of the cough central motor pattern (5, 6, 9). BOT / pre-BOT neuronal clusters of E-DEC, E-AUG early, and E-AUG late neurons shape the activity during cough expiration (5, 9, 10). The activation of the E-DEC units during cough promotes the inspiratory termination. This activity also slightly shifts the activation of a subset of E-AUG BOT neurons known as E-AUG early neurons. E-AUG early units provide excitatory drive to premotor and motor neurons during the cough expulsion (5, 9, 11, 12). The reciprocal inhibition of E-DEC neurons by E-AUG early neurons results in disinhibition of the E-AUG late neurons. These are involved in the termination of active cough expiration by suppressing the E-AUG early units that drive the cough expulsion. Even selective excitation (or inhibition) of one of these neuronal populations can cause significant changes in breathing and coughing. According to the model of Shannon et al. (5, 9), the excitation of E-DEC and / or E-AUG late neurons should result in an attenuated cough.

Several studies (11, 13, 14, 15, 16, 17, 18) reported the effects of neuronal excitation in various regions of rostral VRC by a non-specific glutamate receptor agonist D,L-homocysteic acid (DLH). DLH microinjections to the area of BOT led to a reduction of respiratory rate up to the complete apnoea and reduced amplitudes of inspiratory neuronal and nerve discharges. Higher doses of DLH also increased the expiratory motor discharge (11,13). The present study attempted to verify the ability of computer model to simulate spatiotemporal characteristics of quiet breathing and cough modulated by simulated microinjections of DLH to the BOT area.

METHODS

We observed a simulated influence of a DLH microinjection into the BOT on quiet breathing and cough reflex by a computer model of the generator of quiet breathing and cough developed at the University of South Florida (8). The simulations were performed on a personal computer with the operating system Debian 7.3 64-bit. The control simulations were executed on the model *Control_v33* (19). Integrated signals from neuronal populations innervating main respiratory motor neurons Phrenic and Lumbar were obtained from the simulations. We analysed the durations and the amplitudes of pre-phrenic and pre-lumbar activities during quiet breathing and the cough reflex and the number of coughs elicited by a 10-second-long simulated stimulation. The simulated response was considered to be a cough, when increased the pre-phrenic activity immediately followed by a pre-lumbar activation. The excitation to neuronal, putatively BOT, populations of E-AUG early, E-AUG late (discharging during latter part of the expiratory phase), and E-AUG cough was provided by an additional excitatory fibre population targeting these cells. The excitation "DLH1" represented the excitation by a higher number of fibres and terminals and by the lower synaptic strength, the excitation "DLH2" represented the excitation by a lower number of terminals and by a higher synaptic strength (Table 1). The synaptic connections from DLH excitatory populations to all 3 target E populations had the same parameters (Table 2).

Table 1 Parameters of fibre populations in 2 levels of DLH excitations

Level of excitations	PF	TBF [steps]	TEF [steps]	FP
DLH1	0.07	0	200000	150
DLH2	0.07	0	200000	50

Abbreviations: PF – probability of firing, TBF – time to begin firing, TEF – time to end firing, FP – fibres in populations.

Table 2 Parameters of synapses coming from DLH population

Level of excitation	MinCT [steps]	MaxCT [steps]	NT	SS	ST
DLH1	0	3	150	0.01	Exc
DLH2	0	3	50	0.12	Exc

Abbreviations: MinCT – minimum conduction time, MaxCT – Maximum conduction time, NT – number of terminals, SS – synaptic strength, ST – synapse type, Exc – excitation synapse.

One simulation lasted 100 s (200 000 simulation steps, each 0.5 ms). Three cough stimulations (the simulated cough was elicited by a cough driving fibre population targeting appropriate neuronal populations, 5) with 10 seconds durations and 10 – 15 seconds separations were performed in each simulation. The analysed data are expressed as means ± SE. ANOVA with Student-Newman-Keuls post-tests, paired and unpaired t-test were used in the statistical analysis as appropriate. The changes of the parameters were considered to be significant if $p < 0.05$.

RESULTS

The simulations confirmed several times higher amplitudes of the pre-phrenic activation during coughs compared to the breathing (Table 3) at all 3 levels of excitatory drive to the putative BOT neurons. The additional excitation (DLH1, DLH2) resulted in a reduced pre-phrenic activity during breathing (Table 3).

The respiratory rate was significantly increased during the DLH1 as well as the DLH2 simulated excitations (Table 3). No significant differences were found for the duration of pre-phrenic activation during breathing and that for coughing on a different level of BOT excitation (Table 3). However, the durations of inspiratory cough activity were markedly shorter than the durations of quiet breathing inspirations (Table 3).

The simulated excitations of the BOT neurons (DLH1, DLH2) reduced the pre-lumbar activity that was present in the control simulated coughs and reduced their number (Table 3, Fig. 1). The duration and the amplitude of lumbar cough activity in the DLH1 and DLH2 BOT excitation was reduced (Table 3). Despite this significant difference in the duration of cough pre-lumbar activity, the entire cough cycle durations remained stable (Table 3).

Table 3 Average values of duration and amplitude of activity from the pre-phrenic and pre-lumbar neuronal populations during quiet breathing and cough.

	Control	DLH1	DLH2
RR [breaths / min]	16.08±0.13	17.9±0.08[+]	20.12±0.25[+]
QB Phr Ampl [%]	16.1±0.8	12.8±0.5[+]	13.5±0.5[+]
QB Phr Dur [%]	465.7±11.4	460±14.3	454.3±11.4
QB Lum Ampl [%]	22.7±0.7	0[#]	0[#]
QB Lum Dur [%]	431.4±25.7	0[#]	0[#]

Continuation of table 3

CN	13.2±0.2	4.8±0.37[++]	0.55±0.24[++]
Cough Phr Ampl [%]	100±3.9[*]	104.6±4.5[*]	103.8±4.2[*]
Cough Phr Dur [%]	100±5.7[***]	82.9±8.6[***]	82.9±5.7[***]
Cough Lum Ampl [%]	112.5±8.4[***]	13.3±3.8[+++]	7±1.9[++]
Cough Lum Dur [%]	68.6±5.7[***]	25.7±5.7[+++]	8.6±5.7[+++]
CTtot [%]	202±14.9	164.8±8.6	174.8±10.3

Abbreviations: RR – respiratory rate (breaths / min); QB – quiet breathing; Phr – pre-phrenic and Lum – pre-lumbar neronal populations; Ampl – amplitude; Dur – duration; CN – cough number per 10 s stimulation; CTtot – the whole cough cycle duration, all amplitudes (signal voltage) and durations are expressed relative to Phr during control coughs; QB vs. Cough, * $p<0.05$, ** $p<0.01$, *** $p<0.001$; Control vs. DLH, [+] $p<0.05$, [++] $p<0.01$, [+++] $p<0.001$; # - statistically not evaluated due to no pre-lumbar neuronal activity.
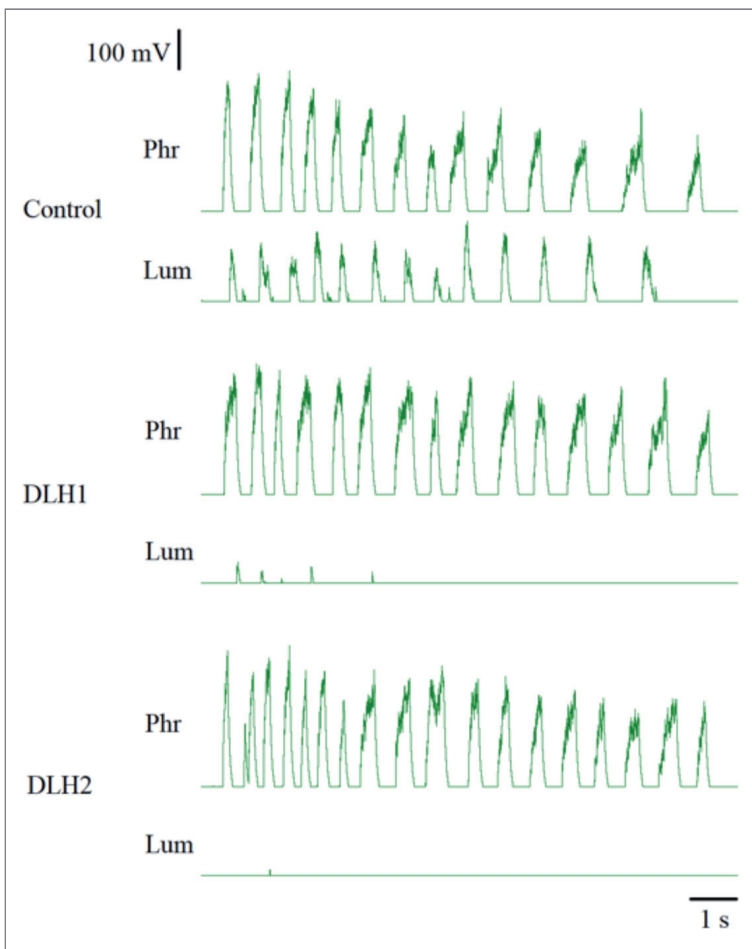

Fig. 1 Activities from the pre-phrenic (Phr) and pre-lumbar (Lum) neuronal populations during cough in control, DLH1 and DLH2 simulated excitation. (Source: author)

DISSCUSION

The main result of our simulations is that the cough reflex was attenuated by a simulated excitation of neurons in the BOT. The results are consistent with the animal experiments where the microinjections of DLH were performed to the BOT area (17, 18). The attenuation of the cough was manifested as a decrease in the number of coughs and a decrease of neuronal activity to the lumbar cell population during cough cycles. Poliacek et al. (17) microinjected DLH, a non-specific glutamate receptor agonist, into the BOT area characterized by the presence of a multi-unit expiratory augmenting activity. DLH microinjections in cats decreased the cough number and the cough abdominal muscles activity similar to the simulations.

The model employed in our simulations is capable to generate simulated coughs (5, 6, 19). In order to mimic BOT neuron excitation, 3 populations of expiratory neurons in the model were driven by the excitatory fibre population (simulating the DLH microinjections in cat). Poliaček et al. (17) reported reduced inspiratory efforts during tracheobronchial stimulation after a DLH microinjection into the BOT region (during coughs and cycles without abdominal activity compared to the pre-microinjection cough controls). In our simulations, we did not observe significant changes in the amplitude of the cough pre-phrenic activity on any level of simulated DLH excitation. Consistently with the experimental study (17), the excitation of the BOT expiratory neurons did not change the duration of inspiratory cough activity. However, in the simulations, the duration of the cough pre-phrenic activity was strikingly shorter compared to the pre-phrenic activities during a quiet breathing (Table 3). Such difference in the inspiratory activation between the cough and the breathing was not observed in cat experiments (17). These facts mean that the model of respiratory and cough neuronal network increases the activity of the inspiratory motor output due to a simulated cough stimulation in the similar manner as shorter this activity. The discrepancy between the experiment (where the duration of the inspiratory activity is similar) and the simulations results from the properties of the model. The model is surely simplified relative to real neuronal connectivity and omits the number of in vivo control elements. Their supposedly "stabilizing" effects on the generator network could result also in a transient suppression of breathing in vivo (17), while there is a slight increase in the respiratory rate in the simulations. Moreover, in simulations the BOT excitation provides a stable signal to selected neuronal populations, while in vivo DLH microinjections cannot ensure such condition (the DLH excitation varies over the time and unequally affects all the types of neuron in the area). Immediately after the DLH microinjections in cats, brief apnoea occurred with gradual recovery of respiration and return of respiratory rate to the pre-microinjection values. The lower breathing amplitude of pre-phrenic activity after simulated BOT excitation is consistent with the experimental work (14, 17). However, this decrease in cat was transient for approximately one minute after the DLH microinjection (17).

Commonly reduced cough number and the cough expiratory motor output were observed in both simulations (Table 3) and cat experiments (17). However, the shortening of the pre-lumbar cough activity in simulations of the BOT excitation was apparently higher than the shortening of the cough abdominal discharge in vivo (17). This extreme sensitivity of the cough phase durations to the excitatory / inhibitory drives in the model neuronal populations results from model simplifications and might be corrected in future versions of the model.

The temporal "stability" of the breathing / cough cycles generated by the respiratory and cough neuronal network and mostly also inspiratory burst duration is given by the activity of the I-DRIVER neuronal population (20). Despite the discrepancies in the duration of respiratory vs. cough cycle in simulations, the changes in total breathing cycle and the cough cycle durations after the BOT neurons stimulations are limited in vivo (17) and in simulations (Table 3). The increased activation of putative BOT populations resulted primarily in the changes in amplitudes of motor output (Table 3, 17). Our simulations, consistently with

experimental data (17), are in agreement with the dominance of inhibitory projections from the E-DEC and the E-AUG neurons in the respiratory / cough generating network. Stimulation of these neuronal populations reduce the E-AUG activation of early (excitatory) neurons driving the expiratory motor output (lumbar population, 19, 21).

The model of breathing and cough generator version Control_v33 used in our simulations was built on experimental data of neural *in vivo* recordings. Our results confirm the functionality of the model not just under basic control conditions, but also for analysis of the respiratory and cough responses when the excitability and the activity of neuronal populations are altered. The revealed differences from the experimental data may lead to the tuning and improvement of the model.

Acknowledgements

REFERENCES

1. Merrill EG, Lipski J, Kubin L, Fedorko L. Origin of the expiratory inhibition of the nucleus tractus solitarius inspiratory neurones. Brain Res 1983; 263: 43–50.
2. Ezure K. Synaptic connections between medullary respiratory neurons and considerations on the genesis of respiratory rhythm. Prog Neurobiol 1990; 35: 429–450.
3. Jiang C, Lipski J. Extensive monosynaptic inhibition of ventral respiratory group neurons by augmenting neurons in the Bötzinger complex in the cat. Exp Brain Res 1990; 81: 639–648.
4. Manabe M, Ezure K. Decrementing expiratory neurons of the Bötzinger complex. I. Response to lung inflation and axonal projection. Exp Brain Res 1988; 72: 150–158.
5. Shannon R, Baekey DM, Morris KF, Lindsey BG. Ventrolateral medullary respiratory network and a model of cough motor pattern generation. J Appl Physiol 1998; 84: 2020–2035.
6. Shannon R, Baekey DM, Morris KF, Li Z, Lindsey BG. Functional connectivity among ventrolateral medullary respiratory neurones and responses during fictive cough in the cat. J Physiol 2000; 525: 207–224.
7. Jakuš J, Tomori Z, Stránsky A. Neuronal determinants of breathing, coughing and related motor behaviours : basics of nervous control and reflex maechanisms. Martin : Wist; 2004.
8. Balis UJ, Morrris KF, Koleski J, Lindsey BG. Simulations of a ventrolateral medullary neural network for respiratory rhythmogenesis inferred from spike train cross-correlation. Biol Cybern 1994; 70: 311-327.
9. Shannon R, Baekey DM, Morris KF, Nuding SC, Segers LS, Lindsey BG. Production of reflex cough by brainstem respiratory networks. Pulm Pharmacol Ther 2004; 17: 369–376.
10. Bolser DC, Poliacek I, Jakus J, Fuller DD, Davenport PW. Neurogenesis of cough, other airway defensive behaviors and breathing: a holarchical system? Respir Physiol Neurobiol 2006; 152: 255–265.
11. Bongianni F, Corda M, Fontana G, Pantaleo T. Expiration-related neurons in the caudal ventral respiratory group of the cat: influences of the activation of Bötzinger complex neurons. Brain Res 1990; 526: 299–302.
12. Bongianni F, Mutolo D, Fontana GA, Pantaleo T. Discharge patterns of Bötzinger complex neurons during cough in the cat. Am J Physiol 1998; 274: 1015–1024.
13. Bongianni F, Fontana G, Pantaleo T. Effects of electrical and chemical stimulation of the Bötzinger complex on respiratory activity in the cat. Brain Res 1988; 445: 254–261.
14. Bongianni F, Corda M, Fontana GA, Pantaleo T. Excitatory and depressant respiratory responses to chemical stimulation of the rostral ventrolateral medulla in the cat. Acta Physiol Scand 1993;148: 315–325.

15. McCrimmon DR, Monnier A, Hayashi F, Zuperku EJ. Pattern formation and rhythm generation in the ventral respiratory group. Clin Exp Pharmacol Physiol 2000; 27: 126–131.
16. Poliacek I, Corrie LW, Wang C, Rose MJ, Bolser DC. Microinjection of DLH into the region of the caudal ventral respiratory column in the cat: evidence for an endogenous cough-suppressant mechanism. J Appl Physiol 2007; 102: 1014–1021.
17. Poliacek I, Corrie LW, Rose MJ, Wang C, Bolser DC. Influence of microinjections of D,L-homocysteic acid into the Botzinger complex area on the cough reflex in the cat. J Physiol Pharmacol 2008; 6 (6): 585-96.
18. Shen TY, Poliacek I, Rose MJ, Musselwhite MN, Kotmanova Z, Martvon L, Pitts T, Davenport PW, Bolser DC. The role of neuronal excitation and inhibition in the pre-Bötzinger complex on the cough reflex in the cat. J Neurophysiol 2022; 127 (1): 267-278.
19. Poliacek I, Morris KF, Lindsey BG, Segers LS, Rose MJ, Corrie LW, Wang C, Pitts TE, Davenport PW, Bolser DC. Blood pressure changes alter tracheobronchial cough: computational model of the respiratory-cough network and in vivo experiments in anesthetized cats. J Appl Physiol 2011; 111(3): 861-873.
20. Rybak IA, O'Connor R, Ross A, Shevtsova NA, Nuding SC, Segers LS, Shannon R, Dick TE, Dunin-Barkowski WL, Orem JM, Solomon IC, Morris KF, Lindsey BG. Reconfiguration of the ponto-medullary respiratory network: a computational modeling study with coordinated in vivo experiments. J Neurophysiol 2008; 100(4): 1770-99.
21. Miller AD, Nonaka S, Jakuš J, Yates BJ. Modulation of vomiting by the medullary midline. Brain Res 1996; 737(1-2): 51-8.

MEASUREMENT OF BASE TRANSCEIVER STATION EXPOSURE IN THE EXTRA-VILLAGE ENVIRONMENT- A PILOT STUDY

MISEK JAKUB[1], LAPOSOVA SIMONA[2], HAMZA SLADICEKOVA KATARINA[1], JAKUSOVA JANKA[3], PARIZEK DANIEL[1], JAKUSOVA VIERA[4], VETERNIK MARCEL[1], JAKUS JAN[1]

[1]Department of Medical Biophysics, Jessenius Faculty of Medicine in Martin, Comenius University in Bratislava, Martin, Slovak Republic
[2]Department of Electromagnetic and Biomedical Engineering, Faculty of Electrical Engineering and Information Technology, University of Zilina in Zilina, Slovak Republic
[3]Department of Pathological Physiology, Jessenius Faculty of Medicine in Martin, Comenius University in Bratislava, Martin, Slovak Republic
[4]Department of Public Health, Jessenius Faculty of Medicine in Martin, Comenius University in Bratislava, Martin, Slovak Republic

Abstract

In recent years, communication using electromagnetic (EM) radiation became an integral part of our lives. As a result, there is a large number of base transceiver stations (BTSs) which act as a source of high EM exposure for inhabitants mainly in the "hot-spot" areas. They employ higher values of radiation, thus, providing potentially harmful effects on living or working environment. The aim of this pilot study was to study a distribution of hot-spots and EMF power in a vicinity of BTSs. BTS was located in an extra-village area at least 500 m away from the nearest city or surrounded villages in the district of Martin. The targeted area of EM radiation from the BTS was divided into two smaller zones, the right and the left. For a better visualization, topographic maps were created. Using spectral analyzer Aaronia Spectran HF-6085, intensities of EMF within the frequency range from 880 – 960 MHz (GSM900) were recorded. Maximum values of EMF power flux density were 146.827 $\mu W/m^2$ in horizontal and 96.448 $\mu W/m^2$ in vertical plane. Minimal values were 0.052 $\mu W/m^2$ in horizontal and 0.179 $\mu W/m^2$ vertical plane respectively. The maps revealed two hotspots in the left zone and also two (smaller and larger) hotspots in the right zone. Our values were below the actual limits given by the Slovak Republic and the International Commission for Non-Ionizing Radiation Protection (ICNIRP) safety guidelines. However, the values from the hotspots were above the limits suggested by the BioInitiative Report. Our results indicate an elevation of EMF values in the hot-spots even in the extra-village areas. Further studies are needed to analyze in detail EMF parameters in the hot-spots, and their effects on living and working environments.

Key words: BTS, Hot-spot, Environment exposure, Mobile communication, Cell phone

INTRODUCTION

Mobile communication based on electromagnetic (EM) radiation became an integral part of our lives. The increasing number of cell phones had recruited in a plenty of base transceiver stations (BTSs) covering ongoing calls, especially in cities. Detrimental effects of electromagnetic fields (EMF) on humans and animals are still on debate. In addition to cell phones some reports (1, 2) are concerned with a harmful effect of EMF radiation by BTSs.

The cell phone has a power 0.2 – 2 W but is held close to the body (zero to couple of centimeters). In comparison, BTSs use a higher radiation power (up to 100 W) (3) but they are placed far off the inhabitants (hundreds of meters). However, BTS built in human living environment may result in a higher EM exposure mainly in the "hotspot" areas. The term hotspot means a small land area with an uneven distribution of EMF. It contains the highest values of EMF, thus providing potentially harmful effects on living or working environment. Poor BTS design related to spatial EMF distribution may yield to high exposure values (4). A great uneven distribution of the radiofrequency (RF) field was found in the hotspots when BTSs were built at lower altitudes toward to pedestrians' heads. In this case, the spatial average of intensity (12.1 V/m) has increased to the maximal value 31.6 V/m, i.e. about 2.6-fold increase in EMF. Another example may be provided by the study comparing low and high exposure apartments (5). The high exposure apartment exhibited high RF radiation from nearby base station. The BTS was located only 6.16m from a balcony where outdoor RF EMF values reached up to 6 V/m. For comparison, a measurement was made in the low exposure apartment at the balcony facing to the building with BTS at a distance of approximately 40 m. Here, the maximum outdoor field of 0.75 V/m was measured (about 8-fold less EMF).

A review by Khurana et al. (6) found neurobehavioral effects in 7 out of 10 studies and three of them have documented an increased risk of cancer for population living closer than 500 m from the BTS. An interesting fact is that none of these studies have reported EMF levels above the accepted international guidelines.

Study groups concerning the effects of RF EMF exposure on heart rate variability (7,8,9) found an increased activity of parasympathetic nervous system after exposure to limit intensity values of RF radiation. The research group (8 and 10) also provided the histological results from the rabbit´s cerebellum showing an accumulation of the ferritin aggregates in the tissue even after an acute exposure to EMF.

The authors (11, 12, 13, 14) reported that a low frequency (LF) EMF can have an inhibitory effect on the growth rate and multiplication of the yeast Saccharomyces cerevisiae. They proposed the ion parametric resonance theory as the cause of the observed effects. Experiment results indicate a frequency-dependent proliferative response of both wild-type yeast strands.

Our previous study analyzing the urban and rural microenvironments for E-field (vector of electric field intensity) distribution (15) showed that all measured values were below the legal limits of the Slovak Republic and the International Commission for Non-Ionizing Radiation Protection (ICNIRP) safety guidelines (16). However, the BioInitiative Report from 2012 updated in 2020 (17) judges the adequacy (or inadequacy) of the existing ICNIRP and IEEE C95.1 RF standards. It presents a solid scientific and public health policy assessment that is evidence-based resulting from a current international research and scientific discussion. Thus, all measured values were above this scientifically derived limits.

Because this incongruity the aim of this study was to analyze the EMF field distribution and a possibility of hot-spots appearance in the vicinity of BTS in an extra-village area.

METHODS

Base station

The chosen BTS was located in an extra-village area in order to eliminate the reflections from the buildings and other obstacles located in urban areas. It was built at least 500 m away from the nearest city of Martin and surrounding villages of Dražkovce and Tomčany (the district of Martin) with GPS coordinates N 49.05527˚ E 18.94277˚.

Generally, BTS consists of several antennas radiating signal to various directions, with a proper intensity and frequency, as required. Based on the orientation to the north (azimuth), the selected area was divided into two smaller zones-the right and the left. The

right zone was oriented to the village of Tomčany whereas the left zone was oriented to the city of Martin. By GPS (Global Positioning System) device Garmin Etrex Legend (USA), each point where the E-field was measured was assigned with GPS coordinates and drawn into the map (Fig. 1). The base station corresponded to the zenith point with the coordinates [0, 0]. From the zenith, with respect to the north, the positions were measured in the range of 180°. Based on the azimuth, which was 80˚, the first measurement point was determined. Subsequently, the measurements were made at other points in the same way. Thus, totally 31 positions were measured, of which 17 on the right zone and 14 to the left zone in accordance with the guidelines of ICNIRP (16).

Setup of EMF measurement

The intensity of radiated signal from the BTS was measured by a spectrum analyzer Aaronia Spectran HF-6085 (Germany). The analyzer was able to proceed RF EMF within the frequency range of 10 MHz – 8 GHz. It was completed by a fitted Aaronia HyperLog6080 (Germany) antenna using direct connection. The antenna was held 1.5m above the ground during the measurement. The analyzer was connected to a laptop *via* USB with a pre-installed high frequency recording software compatible with the Aaronia Spectran. The setup allowed to analyze E-field within the frequency range of 880 – 960 MHz, which corresponds to the GSM900 frequency band representing the worldwide standard for mobile communication. All values were measured in the horizontal and vertical planes to catch both polarizations of EMF. During the measurements all cell phones kept by service persons were switched off in order to prevent an addition of false EM intensity.

Topographic maps

To visualize EMF distribution, topographic maps were created in the MATLAB programming environment. Generally, topographic maps represent relief visualization based on the lines or colors. By GPS coordinates, the measurement points were transferred to a cartesian coordinate system and subsequently to the map. The distances between the BTS and the individual measuring points as well as their azimuths were also determined from the GPS records.
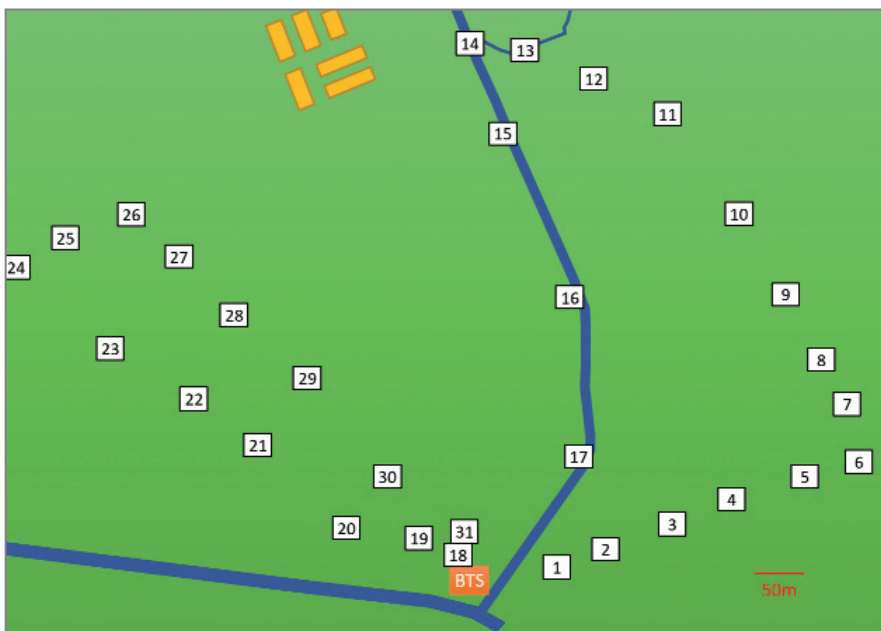

Fig. 1 Schematic representation of extra-village measurement spots showing right (numbers 1-17) and left (numbers 18-31) "zones". Blue lines represent roads and orange color represents buildings. Each square box corresponds to the measurement with a particular number.

RESULTS

The proposed results represent the total EMF power [W/m²] as an arithmetic mean and a standard error of mean ± within the whole frequency range. All results are given in the Tab. 1, showing the number of the measurement which corresponds to numbers in the topographic maps in either horizontal or vertical plane. The results are enounced in the form of average as RMS (Root Mean Square), but not as the maximal values. All measured values (n = 31) were found to be below the valid limits of the Slovak Republic and the ICNIRP safety guidelines. The highest E-field was measured in the left zone (oriented closer to the city). Maximum values were 146.827 (µW/m²) in horizontal and 96.448 (µW/m²) in vertical plane. Minimal values were 0.052 (µW/m²) in horizontal and 0.179 (µW/m²) vertical plane, respectively. Mean value for the first zone was 5.710 ± 1.937 (µW/m²) for horizontal and 10.859 ± 2.929 (µW/m²) for vertical plane. Mean value for the second zone was 15.483 ± 10.373 (µW/m²) for horizontal and 9.576 ± 6.584 (µW/m²) for vertical plane. One of the reasons why the values are so low is that the measurements were taken on the ground relatively close to the BTS.

Tab. 1 Table showing EMF power in the horizontal (1–17) and vertical plane (18–31)

Measurement no.	Distance from BTS [m]	Horizontal [µW/m²]	Vertical [µW/m²]
1.	71	6.1	5.9
2.	113	4.2	5.9
3.	180	5.9	2.8
4.	228	5.4	5.4
5.	316	5.4	5.9
6.	370	5.9	4.2
7.	375	5.6	43.0
8.	377	5.6	41.0
9.	398	4.3	8.0
10.	440	1.0	3.3
11.	503	0.7	6.0
12.	515	0.7	11.4
13.	532	3.3	8.7
14.	530	0.2	2.8
15.	431	36.5	20.6
16.	276	1.0	5.9
17.	140	5.4	4.0
Average I		5.7	10.9
SEM		1.9	2.9

Continuation of table 1

18.	14	2.2	2.0
19.	56	0.8	0.5
20.	117	53.2	96.4
21.	234	0.3	0.7
22.	295	1.1	2.0
23.	390	0.4	0.6
24.	515	0.1	0.3
25.	501	146.8	20.6
26.	473	0.5	0.7
27.	405	2.3	1.1
28.	325	2.3	2.2
29.	235	0.4	0.8
30.	113	0.3	0.2
31.	22	5.9	5.9
Average II		**15.5**	**9.6**
SEM		**10.4**	**6.6**

BTS – base transceiver station, SEM – standard error of mean

The four presented maps illustrate the left (Fig. 2) and the right (Fig. 3) zones, each for horizontal and vertical plane, where the corresponding colors express the level of the measured EMF power. The maps show two hot-spots in the left and two (smaller and larger) hot-spots in the right zone (depicted in a red color). For a better visualization, the color scheme is shown on a logarithmic scale.
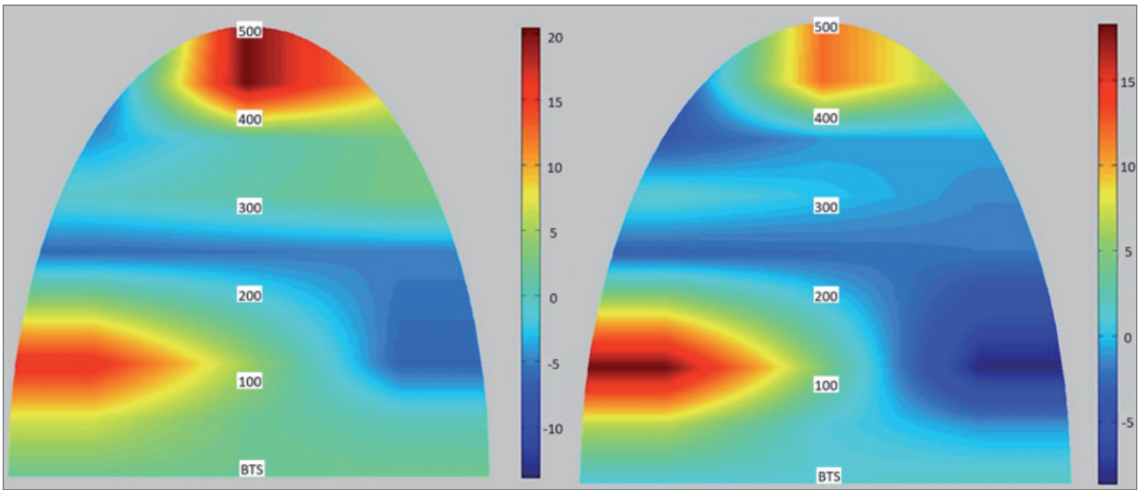
Fig. 2 Topographic map of horizontal (LEFT) and vertical plane (RIGHT) of the left zone with the distance from the BTS given in meters. The color scheme is depicted in a logarithmic scale (log [μW/m2]).
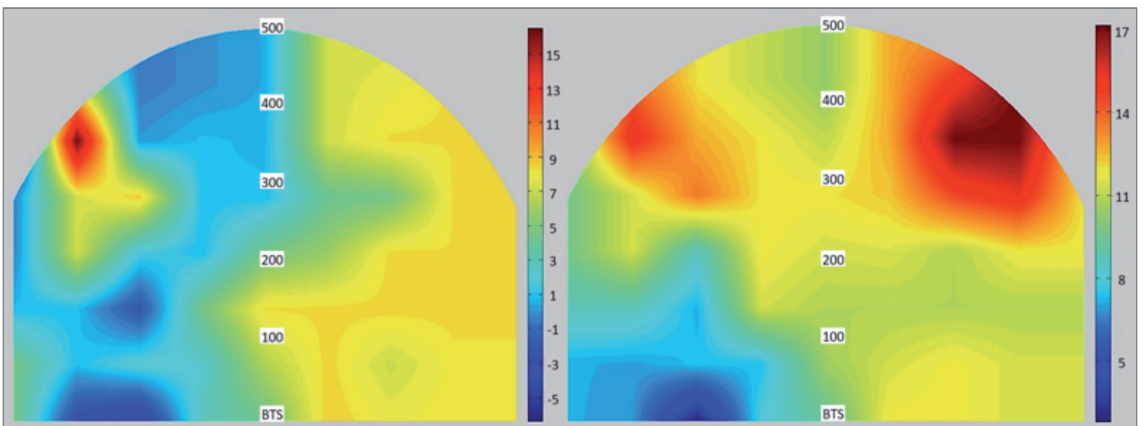

Fig. 3 Topographic map of horizontal (LEFT) and vertical plane (RIGHT) of the right zone with the distance from the BTS given in meters. The color scheme is depicted on a logarithmic scale (log [μW/m2]).

DISCUSSION

The aim of this pilot study was to bring a picture on density of the hotspots nearby the BTS. Our goal was not to measure a complex spectrum of the signal frequencies and E-field intensities, but we wanted to map one particular area and the appearance of hotspots in the vicinity of a BTS in an extra-village environment. Hotspots, as small zones with a high EMF power flux density, are clearly visible on the presented maps with an interesting EMF distribution. The maximum value found in the horizontal plane (no. 24) was located only 49 meters from the minimum in the same plane (no. 25). The EMF power flux density in no. 25 was higher more than 2500-times compared to no. 24 distanced about 550 m from the BTS. A similar situation was observed in the vertical plane where the maximum (no. 20) and the minimum (no. 30) zones where located only 60 m from each other and around 125 m from the BTS (500-fold higher value). These findings confirmed our hypothesis that even in

an extra-village area, where the number of the land obstacles is minimal, EMF was high and unevenly distributed in a form of the hot-spots.

Generally, the exposure to RF EMF was classified as a possible cancer agent (group 2B) both by ICNIRP and WHO (18). ICNIRP established the guidelines in 1998 and had considered only thermal effects of EMF. Even after its update in 2009 no changes were made in the limit values. For the frequency band of 400 – 2000 MHz the limit radiation power flux density remained at $2 – 10$ W/m^2. Nevertheless, the updated BioInitiative Reports for 2012-2020 (17) established the scientific derived limits for possible health risks from $30 – 60$ µW/m^2. In accordance to this, all our measurements were below the present limits of both ICNIRP and the Slovak Republic. However, the values mainly those from the hotspots, exceeded the scientific derived limits given by the BioInitiative Reports.

Our former study focused on the E-field levels taken from different microenvironments (15). At extra-village areas for GSM900 frequency band, we found the total average value of E-field intensity 0.01 V/m (0.26 µW/m^2). However, in this study the location of the extra-village area was at least 1000 m away from the BTS. Thus, comparing these results, the rural environment was considered, where the BTS location was approximately 100 m away. Suggesting only GSM900 component a total average of E-field intensity in rural was 0.13 V/m (44.83 µW/m^2). Thus, these results are along with our present findings.

In a recent study, Koppel et al. (4) measured BTS parameters when the antennas were placed at lower positions closer to pedestrians' heads. They found the highest value of spatial average across all cells 388 mW/m^2, whereas the maximum reading from the entire area was 2648 mW/m^2. The reason why these values are higher compared to our study could be explained by not including the higher frequency bands which the study group reported as the highest (e.g. 2100 and 2600 MHz used for 3G and 4G technologies). The mentioned paper also proposed the results that show a highly uneven distribution of RF fields creating hotspots, suggesting poor design of BTSs. Sogut et al. (19) measured the level of EM pollution in the city. They brought the results from three major frequency bands GSM900, GSM1800, and UMTS2100. Along one street they also found high variations in intensity of the signal, i.e. for GSM900 band the lowest average value was 1.49 (µW/m^2) and the highest 1159.1 (µW/m^2), thus confirming the miscellaneous spread of EMF.

The study of Hardell et al. (20) provided information on the RF EMF exposure in the Old Town of Stockholm. They found large contrasts between the areas with the highest (mean: 24 277 µW/m^2, min. 257 µW/m^2 and max. 173 302 µW/m^2) and the lowest (404 µW/m^2, min. 20.4 µW/m^2 and max. 4 088 µW/m^2) power flux density. Compared to our study, their maximum values far exceed our results. The authors mentioned that some antennas were located significantly closer to humans, sometimes only a few meters from the ground level, while our study focused on the BTS in the extra-village environment and only for a short frequency band. Anyway, their study clearly showed a large variation in the outdoor RF radiation level.

Since hotspots are not visible and cannot be detected by any other methods except of detailed measurement of the selected area, Aerts et al. (21) brought a novel methodology to create the heat maps that accurately pinpoint the outdoor locations with an elevated exposure in the hotspots. By computer simulation a surrogate model could be built from the available data using a kriging-based sequential sampling. Based on the simulation strategy, new measurement locations can be selected at spots which are deemed to contain the most valuable information inside the hotspots. They verified totally 650 measurements and had found 5 hotspots in the urban area of approximately 1km^2. The mentioned findings, including ours, may support the theory of the hot-spots appearance with a potentially harmful elevation of EM radiation for living environment. Thus, more attention should be paid to this issue since a progressive rise of EMF exposure is reported from many countries (e.g. 22, 23).

As EMF exposure from BTSs is perceived as a part of our living environment, it cannot be easily eliminated. To ensure a new generation of 5G networks and other telecommunication

services, new BTSs are built at new locations, thus increasing the total annual exposure of inhabitants (20). By this study we highlight monitoring of the base stations whether in the cities or outside with a determination of hot-spots and their possible detrimental effects to humans living and working in the vicinity.

The limitation of the present pilot study is a relatively small number of measurements. We are aware that our short-term measurements did not involve the changes in BTS radiation during a day or a week as reported in literature (24). For future studies, multiple measurements at wider frequencies must be employed.

CONCLUSION

The aim of this pilot study was to analyze the field distribution and create their topographic maps in the vicinity of BTS located in an extra-village area. Our findings showed that even in the extra-village area, where the number of the spatial obstacles are rare, EMF could be highly and unevenly distributed in hot-spots. Our topographic maps revealed four hotspots in the vicinity of one BTS. Since the number of BTSs will progressively rise up, more attention should be paid to the detrimental effect of EM radiation from hot-spots on living environment. All our measurements were below the present limits of both ICNIRP and the Slovak Republic. However, the values mainly those from the hotspots, exceeded the scientific derived limits given by the BioInitiative Reports.

REFERENCES

1. Belyaev I., Dean A., Eger H., Hubmann G., Jandrisovits R., Kern M., Kundi M., Moshammer H., Lercher P., Müller K., Oberfeld G., Ohnsorge P., Pelzmann P., Scheingraber C., Thill R. EUROPA-EM EMF Guideline 2016 for the prevention, diagnosis and treatment of EMF-related health problems and illnesses. Rev Environ Health 2016; 31(3): 363–397.
2. Koricarova S. Measurements of exposure levels of mobile providers base stations. *Bachelor thesis. [In Slovak]* Zilina: s.n.; 2014. p.31
3. Akinyemi L.A., Makanjuola N. T, Shoewu O., Edeko F.O. Comparative Analysis of Base Transceiver Station (BTS) and Power Transmission Lines Effects on The Human Body in the Lagos Environs. African Journal of Computing & ICT 2014; 7(2): 33-42.
4. Koppel T., Ahonen M., Carlberg M., Hardell L. Very high radiofrequency radiation at Skeppsbron in Stockholm, Sweden from mobile phone base station antennas positioned close to pedestrians' heads. Environ Res 2022; 208(112627): 1-8.
5. Koppel T., Ahonen M., Carlberg M., Hedendahl L.K., L. Hardell. Radiofrequency radiation from nearby mobile phone base stations-a case comparison of one low and one high exposure apartment. Oncology Letters 2019; 18:5383-5391.
6. Khurana V.G., Hardell L., Everaert J., Bortkiewicz A., Carlberg M., Ahonen M. Epidemiological evidence for a health risk from mobile phone base stations. Int. J. Occup. Environ Health 2010; 16(2010): 263-267.
7. Misek, J., Belyaev, I., Jakusova, V., Tonhajzerova, I., Barabas, J., Jakus, J. Heart rate variability affected by radio frequency electro-magnetic field in adolescent students. Bioelectromagnetics 2018; 39(4): 277-288.
8. Misek J., Veternik M., Tonhajzerova I., Jakusova V., Janoušek L., Jakus J. Radiofrequency electromagnetic field affects heart rate variability in rabbits. Physiol Res 2020; 69(4): 633-643.
9. Parizek D., Sladicekova K., Tonhajzerova I., Veternik M., Jakus J. The Effect of Music on Heart Rate Variability (Review). Acta Medica Martiniana 2021, 21(1): 1-8.
10. Kopani M., Filova B., Sevcik P., Kosnac D., Misek J., Polak S., Kohan M., Major J., Zdimalova M., Jakus J. Iron deposition in rabbit cerebellum after exposure to generated and mobile GSM electromagnetic fields. Bratisl Med J, 2017; 118(10): 575-579.

11. Sladicekova K., Bereta M., Misek J., Parizek D., Jakus J. Biological effects of a low-frequency electromagnetic field on yeast cells of the genus Saccharomyces Cerevisiae. Acta Medica Martiniana, 2021, 21(2): 34-41.
12. Barabas J., Radil R., Malikova I. Modification of S. cerevisiae growth dynamics using low frequency electromagnetic fields in the 1-2 kHz range. Biomed Res Int 2015; 2015: 1-5,
13. Radil R., Barabas J., Janousek L., Bereta M. Frequency Dependent Alterations of S. Cerevisiae Proliferation Due to LF EMF Exposure. Advances in Electrical and Electronic Engineering 2020; 18(2), 99 – 106.
14. Barabas J., Radil R. Evidence of S. Cerevisiae Proliferation Rate Control via Exogenous Low Frequency Electromagnetic Fields. In: Information Technologies in Biomedicine. Itib 2012, 7339: 295-303. Springer, Berlin, Heidelberg.
15. Misek J., Laukova T., Kohan M., Veternik M., Jakusova V., Jakus J. Measurement of Low-level radiofrequency electromagnetic fields in the human environment. Acta Medica Martiniana 2018; 18(2): 27-33.
16. ICNIRP. Guidelines for limiting exposure to time varying electric, magnetic, and electromagnetic fields (up to 300 GHz). Health Physics 1998; 74(4): 494–522.
17. BioInitiative Working Group: BioInitiative 2012. A Rationale for a Biologically based Public Exposure Standard for Electromagnetic Fields (ELF and RF). In: Sage C and Carpenter DO, ed. Bioinitiative, 2012. Available online: https://www.bioinitiative.org. [Last Accessed: February 1, 2022].
18. IARC Monographs on the Evaluation of Carcinogenic Risks to Humans, Volume 102. Non-Ionizing Radiation, Part 2: Radiofrequency Electromagnetic Fields. International Agency for Research on Cancer: Lyon, France, 2013.
19. Sogut O., Eyicil M. Measurement of Electromagnetic Pollution Level and Calculation of Radiation Dose Index throughout Malatya Street in Elbistan District of Kahramanmaraş. Journal of Science and Technology 2021; 14(1), 204-214.
20. Hardell L., Carlberg M., Koppel T, Hedendahl L. High radiofrequency radiation at Stockholm Old Town: An exposimeter study including the Royal Castle, Supreme Court, three major squares and the Swedish Parliament. Mol Clin Oncol 2017; 6(4): 462–476.
21. Aerts S., Deschrijver D., Verloock L., Dhaene T., Martens L., Joseph W. Assessment of outdoor radiofrequency electromagnetic field exposure through hotspot localization using kriging-based sequential sampling. Environ Res 2013; 126(2013):184-191.
22. Urbinello D., Joseph W., Verloock L., Martens L., Röösli M. Temporal trends of radio-frequency electromagnetic field (RF-EMF) exposure in everyday environments across European cities. Environ Res 2014; 134(2014):134-142.
23. Sánchez-Montero R., Alén-Cordero C., López-Espí P.L., Rigelsford J.M., Aguilera-Benavente F., Alpuente-Hermosilla J. Long term variations measurement of electromagnetic field exposures in Alcalá de Henares (Spain). Sci Total Environ 2017; 598 (2017):657-668.
24. Aerts S, Wiart J, Martens L, Joseph W. Assessment of long-term spatio-temporal radiofrequency electromagnetic field exposure. Environ Res 2018; 161: 136-43.

CLASSIFIER SPOT COUNT OPTIMIZATION OF AUTOMATED FLUORESCENT SLIDE SCANNING SYSTEM

ZASTKO LUCIAN[1, 2, *], BERETA MARTIN[3], TIMKO JAROSLAV[2, 4] AND BELYAEV IGOR[1]

[1]Department of Radiobiology, Cancer Research Institute, Biomedical Research Center, University Science Park for Biomedicine, Slovak Academy of Sciences, Bratislava, Slovakia
[2]Department of Laboratory Medicine, Faculty of Health Care, Catholic University in Ružomberok, Ružomberok, Slovakia
[3]Department of Radiological Technology, Faculty of Health Care, Catholic University in Ružomberok, Ružomberok, Slovakia
[4]Department of Clinical Microbiology, Central Military Hospital, Ružomberok, Slovakia

Abstract

Purpose: Ionizing radiation induced foci (IRIF) known also as DNA repair foci represent the most sensitive end-point for assessing DNA double strand breaks (DSB). IRIF are usually visualized and enumerated with the aid of fluorescence microscopy using antibodies to γH2AX and 53BP1. Although several approaches and software packages were developed for the quantification of IRIF, not one of them was commonly accepted and inter-laboratory variability in the outputs was reported. In this study, the sensitization of Metafer software to counting also small appearing IRIF was validated. **Materials and Methods:** Human lymphocytes were γ-irradiated at a dose of 2 Gy. The cells were fixed at 0.5, 1, 2, and 18 hours post-irradiation, permeabilized and IRIF were immunostained using appropriate antibodies. Cell images were acquired with the automatic Metafer system. Radiation-induced γH2AX and 53BP1 foci were enumerated using either manual counting (JCountPro program) or the Metafer software (after its classifier optimization has been done) and compared. The statistical analysis was performed using One-way ANOVA.

Results: The enumeration of 53BP1, γH2AX foci manually by JCountPro did not statistically significantly differ from the automatic one performed with the optimized Metafer classifier. A detailed step-by-step protocol of this successful optimization is described in this study.

Conclusions: We concluded that the Metafer software after the optimization was efficient in objectively enumerating IRIF, having a potential for usage in clinics and molecular epidemiology.

Keywords: DNA double-strand breaks; DNA repair foci; ionizing radiation.

INTRODUCTION

DNA double-strand breaks (DSB) are the most detrimental type of DNA damage. The cytological manifestation of DSB induced by ionizing radiation (IR) is a formation of so-called ionizing radiation-induced foci (IRIF) which are also referred to as DNA repair foci (1). The IRIF can be microscopically visualized as discrete foci around DSB. A key event in the IRIF formation is the rapid phosphorylation of histone H2AX (γH2AX) that marks a chromatin scaffold formed on a 2 megabase-sized chromatin domain containing DSB. This domain functions by recruiting proteins involved in DSB repair (2). The γH2AX has beco-

Corresponding author: exonzast@savba.sk; lucian.zastko@ku.sk

me a well-established biomarker for IRIF in low-dose research (3), diagnostic radiology (4 – 6), cancer research and therapy (7), and biological dosimetry (8 – 11). Another established molecular marker of DSB is p53 binding protein 53BP1 (12 – 14). Due to different kinetics of formation and decay, γH2AX and 53BP1 foci do not always co-localize (15, 16). However, co-localized γH2AX/53BP1 foci are commonly considered as the most reliable marker for DSB (17, 18).

Several software/freeware programs were developed and used for automatic IRIF scoring in human cell lines (19 – 27). The majority of studies focus on human lymphocyte because these cells are readily available for different purposes. Computational algorithms designed to identify and count foci operate with a certain number of parameters that need to be specified by the user. Recently, the JCountPro software was verified on the same samples in two independent laboratories for enumeration of γH2AX, 53BP1 foci and their co-localization after irradiation of human lymphocytes with low doses (28). The Metafer slide scanning system (MetaSystems, GmbH, Altlussheim, Germany) classifier sensitization to counting small foci (often falsely considered for background noise) and a consequent comparison to manual counting performed using the JCountPro software has been evaluated in this study.

MATERIALS AND METHODS

Reagent grade chemicals were obtained from Sigma-Aldrich (St. Louis, MO, USA), Merck KgaA (Darmstadt, Germany), and Life technologies (Carlsbad, CA). This study has been approved by the Ethics Committee of Children's Hospital in Bratislava. Umbilical cord blood mononuclear cells (UCB MNC), extracted as previously described (29), from three healthy newborns after full-term pregnancies, were provided by Dr. M. Kubes, Eurocord-Slovakia, Bratislava, Slovak Republic.

Frozen UCB MNC were thawed and diluted in 10 ml of thawing medium containing 4.5 ml of Hanks´ Balanced Salt Solution (HBSS) medium (Gibco, Life Technologies, United Kingdom), 1 ml of 1 mg/ml DNAse I Sigma-Aldrich (St. Louis, MO, USA), (100 µg/ml working concentration), and 4.5 ml of Roswell Park Memorial Institute medium (RPMI) 1640 medium with L-glutamine and 4-(2-hydroxyethyl)-1-piperazineethane-sulfonic acid (Hepes) (PAA Laboratories GmbH, Pasching, Austria). Adherent cells (monocytes) were excluded after 2 hour (h) incubation of cells in 25 ml of basal medium (BM): RPMI 1640 medium, supplemented with 10% fetal bovine serum (FBS), 100 IU/ml penicillin, 100 mg/ml streptomycin (Gibco, Invitrogen, Germany). The viability of remaining umbilical cord blood lymphocytes (UCBL) was not less than 95% as defined by the Trypan blue exclusion assay. After 2 h incubation, UCBL were spun down at 100 g, diluted in 50 ml (approximate cell density of $2x10^6$/ml) of BM, and then divided into 2 aliquots (one to be irradiated and one as a control) and incubated on ice 40 min prior to irradiation. UCBL were irradiated by γ-rays at the dose rate of 0.45 Gy/min with a dose of 2 Gy using the cobalt ^{60}Co - TERAGAM® K-02 source (UJP Praha, Prague, Czech Republic). The dose deviation was below 5%. The already irradiated cells were immediately warmed to 37°C (±0.1°C) in a water bath (ED v.2, Julabo Labortechnik GmbH, Seelbach, Germany) and then incubated at 37°C in a humidified incubator (NB-203XL, N-BIOTEK, Inc., Bucheon, South Korea) at 5% CO_2 for 0.5 – 18 h.

0.5, 1, 2, and 18 h post-irradiation, UCBL were washed with a phosphate-buffered saline (PBS, 3.2 mM Na2HPO4, 0.5 mM KH2PO4, 1.3 mM KCl, 135 mM NaCl, pH 7.4) and spun down using the Shandon Double Cytofunnels (ThermoScientific, Runcorn, Cheshire, UK) on the double cytoslides coated with polysine (ThermoScientific, Menzel-Glaser, Braunshweig, Germany) at 85 g, 5 min using the Cellspin I cytocentrifuge (Tharmac GmbH, Germany). The cells were fixed with 3% paraformaldehyde for 15 min and left in the fridge overnight (for 16 – 17 h). The cells were then permeabilized with 0.2% TRITON X-100 for 5 min, washed extensively with PBS, and blocked in 3% FBS (Gibco, Germany) for 30 min at RT.

The primary antibodies, monoclonal γH2AX antimouse (cat. no. #NB100-78356, Novus Biologicals, United Kingdom) (dilution 1:800) and polyclonal 53BP1 antirabbit (cat. no. #NB100-304, Novus Biologicals, United Kingdom) (dilution 1:1000), were diluted in 3% FBS in PBS and applied in 100 µl aliquots to the slides. The slides were incubated for 1 h in a humidified chamber at RT. After washing with PBS, the secondary antibodies, Alexa Fluor 488 IgG (H+L) polyclonal antirabbit (cat. no. #A11029, Invitrogen Molecular Probes, Life Technologies, USA) (dilution 1:200) and Alexa Fluor 555 IgG (H+L) monoclonal antimouse (cat. no. 21429, Invitrogen Molecular Probes, Life Technologies, USA) (dilution 1:200), were added. Then, the slides were incubated for 1 h in the humidified chamber at RT, washed with PBS, and counterstained with an antifade reagent agent VECTASHIELD (Vector Laboratories, Peterborough, United Kingdom) containing 4',6-diamidino-2-phenylindole (DAPI).

Image acquisition of DSB repair foci were conducted using the Metafer Slide Scanning System V 3.9 and Zeiss Axio Imager.Z2 epifluorescent microscope (Carl Zeiss Microscopy GmbH, Gottingen, Germany).

The comparison between groups for pooled data that fitted normal distribution (analyzing designs with a single categorical independent variable) was performed using a One-way ANOVA test, adjusted by Post-hoc Fisher LSD test. All statistical operations were carried out using the Statistica 8.0 software (StatSoft Inc., Tulsa, OK, USA). The results were considered as significantly different at $p < 0.05$.

RESULTS

The „step-by-step" classifier spot count optimization

One of the focus enumeration problems with the Metafer system is an incomplete small foci counting, which needs to be optimized in order to result transparency, as major portion of small foci are often considered falsely for background noise. We decided to perform this classifier „small foci counting disability repair" operation on lymphocytes from peripheral blood samples and then check the newly optimized classifier functionality on a comparison of UCBL manually (JCountPro) and by Metafer counted γH2AX and 53BP1 levels induced by 2 Gy γ-irradiation. The creation of the new classifier from an existing one to read the initial settings from was the first thing to perform and the following parameters were checked: correct focus parameter set, correct color channels definition, magnification and microscope configuration. Then the training data, used for the new classifier spot count optimization, were recorded – we chose the experiment performed on lymphocytes from peripheral blood, where small foci were induced as a consequence of 0.1 Gy γ-irradiation (data not shown).

Image quality

The next step in the optimization of the new classifier spot count was to check the image quality with respect to the signal background, signal intensity, and integration time and to define, which objects (cells) we wanted the Metafer to detect (this was done at the training images) (Figure 1A). When processing the images in the Metafer MetaCyte software in the lower right corner of the screen the colored squares representing the available color channels are shown. Within the squares of the color channels used, the integration time is displayed. This value should be checked carefully for different image fields: for images with visible signals it should be lower than the maximum integration time that is defined in the corresponding MetaCyte classifier.

Only in empty images or images not showing signals it should be equal to the maximum integration time. Besides the integration time there was also other thing that needed to be checked – the noise background level of the images. If the noise level is too high (granular background), it is difficult or even impossible to optimize the spot counting. In this case the
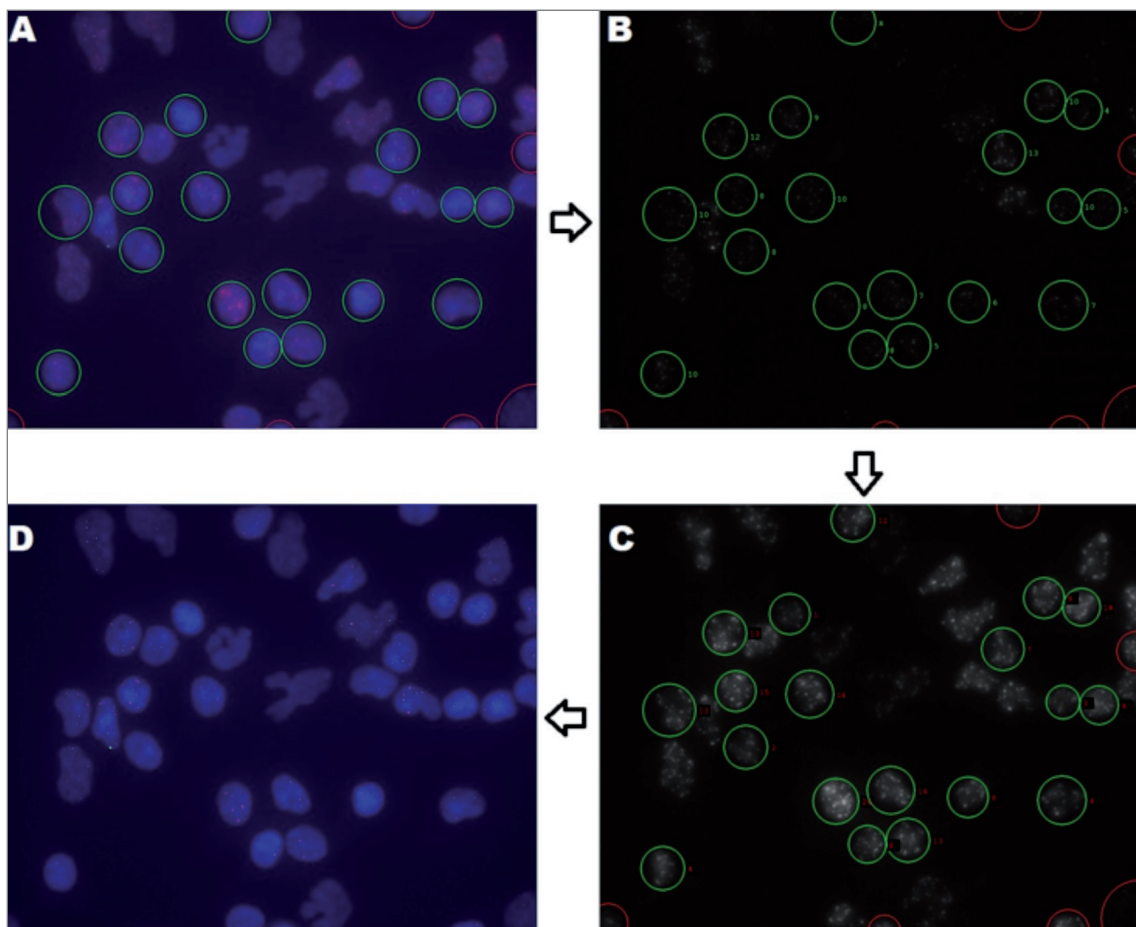
Fig. 1. Training images obtained and processed with the Metafer slide scanning system. **A:** classifying the cells of interest: green circles – the cell of the right morphology, red circles – rejected cells (image before the application of image processing operations); **B:** green numbers in dark squares as well as white spots inside the green circles represent spot counts of 53BP1 foci for each classified positive cell; **C:** red numbers in dark squares as well as white spots inside the green circles represent spot counts of γH2AX foci for each classified positive cell; **D:** training image obtained after the application of sequence of image processing operations (compare with image A).

camera gain could be lowered. Vice versa, if the background level of the images is low but long integration times have been used, the camera gain could be increased. If very bright artifacts seem to interfere with the integration time adjustment and the signal intensities are poor, the following question arises: if the „*Use Counterstain Mask during Capturing?*" option of the corresponding MetaCyte classifier has been enabled. In all cases, where a change of the settings for image capturing is needed, the whole re-capture process of the training data, before proceeding with cell classification and adjustment of image processing operations need to be repeated and recorded again. After obtaining properly captured and recorded training images we classified the cells of interest (of right morphology) as well as cells we wanted the Metafer to reject (cells lying at the border of the classified image) and to exclude from analyses (Figure 1B). The number of classified images reached the amount of nearly 50, the number of classified cells within, used for classifier optimization, reached up to 500.

To optimize the classifier on spot counting, the number of spots of the already classified cells needed to be defined first. The best option here is to adjust the spot count for all positive cells (in green circles), for each color channel separately. The selected color channel of the actual image field will be displayed in black and white, where the number of white spots inside the circle equals the number of foci and the spot count can be defined (Figure 1C). If the spot count for a cell cannot be specified (e.g. granular background or low intensity of spots), there is an option to reject it for only this color channel by selecting „X" as spot count. In this case the cell will not be used for optimizing the spot count in this color channel.

Image processing operations

To increase the image quality and set a lower threshold, thus order the classifier what should be brought to front and counted, image processing operations can be used. The proper set-up-way for their gain is to open the training data and try out and find the best possible sequence, so-called image processing algorithm, from image processing operations (*Background, Mask, Sharpening, Smoothing, Threshold, Gray Levels, Image Buffers,* and *Other*) by applying them to the training images (Figure 1D). Our group, after a careful consideration and countless analyses, decided to use three of them, as these three particularly influenced the overall outcome of the "pre-optimizations" the most – **Background**, **Threshold**, and **Grey Levels**.

• **Background** – By opening this option, the number of all different possible operations is listed. We are using just one of them, *SBLocMinAsy (Subtract background, Local Asymmetric Minimum).* This operation is very efficient in removing a continuous variable background, but produces artifacts if there are discontinuities in the background intensity. If for example the within cell fluorescence background in a signal channel is much higher than the between cell background level, there will be ring shaped artifacts at the nucleus borders. The *SBLocMinAsy* operation avoids this by analyzing the background intensities on all four sides of the current pixel separately and then subtracting the highest of the four values.
• **Threshold** – Here we are making use of *SegThrAbs(X) (Set Absolute Segmentation Threshold at X/1000)* operation that subtracts the segmentation threshold to the specified value. The threshold is specified in units of X/1000 of the available grey level range. To apply the calculated segmentation threshold, where all grey levels less than or equal to the threshold are set to zero, we also chose *ApplySegThr (Apply Current Segmentation Threshold)* operation.
• **Grey levels** – To calculate an upper threshold and then stretch the grey levels between 0 and this threshold to the full available range (0...255), we chose *StretchGL-NSP(X) (Stretch Grey Levels, Number of Saturated Pixels = X)* operation. We set the number of saturated pixels to 10.

Focus parameter set

The number of focus planes of an existing classifier was **7**, the focus plane distance **28/40 µm**, so in order to ensure the scan of the whole cell volume, we increased the number of focus planes of newly created one to **10**, but nothing was changed in the plane distance.

There are 5 parameters for spot counting to be optimized: *Spot Measurement Area (rel./abs.)*, *Min. Spot Distance (rel./abs.)*, *Min. Spot Rel. Intensity (%)*, *Maximum Spot Area,* and *Minimum Spot Contrast*. For the columns *Min.*, *Max.*, and *Step* it is possible to enter values for all 5 parameters before starting the optimization, the *N* values will be updated automatically, the total number of parameter combinations is displayed in the line *Iteration:*. As all 5 spot counting parameters depend on each other, it is best to optimize them

together. We avoided doing an optimization of multiple parameters with wide ranges and small steps at the same time. It is recommended first to find a preliminary optimum using a wide range, but relatively large steps. Then a second optimization around this parameter combination with small steps can be done to find the optimum parameters more precisely.

• The values of an existing classifier focus parameter set: for FITC (53BP1) signal - *Abs. Spot Meas. Area 20/100 µm; Distance 5/10 µm; Intensity 25%*;
   for SpOrange (γH2AX) signal - *Abs. Spot Meas. Area 20/100 µm; Distance 5/10 µm; Intensity 25%*;
   for fusion signals – *Channel Mask 6; Max. Dist. 5/10 µm*

We did not manipulate with *Abs. Spot Meas. Area* parameter value but we did focus more on *Distance* and *Intensity* parameter values instead. The selected classified training data were analyzed with all possible combinations of parameter values specified by the ranges (for both signals: *Distance 1 – 4/10 µm; Intensity 5 – 20%*) and steps for the single parameters.

• The values of the newly optimized classifier focus parameter set: for FITC (53BP1) signal - *Abs. Spot Meas. Area 20/100 µm; Distance 3/10 µm; Intensity 10%*;
   for SpOrange (γH2AX) signal – *Abs. Spot Meas. Area 20/100 µm; Distance 2/10 µm; Intensity 5%*;
   for fusion signals – *Channel Mask 6; Max. Dist. 5/10 µm*

While the optimization was carried out, several fields were simultaneously updated. In the column **Best** the parameter values for the iteration with the smallest error index were displayed. After the first iteration had been finished, the elapsed time and estimated duration of the optimization were displayed. Depending on the size of the training data set, the speed of the computer and the defined number of iterations the classifier optimization would take several hours and therefore had been done overnight.

After the optimization had been finished the values from the column **Best** were transferred to the columns **Min.** and **Max.** and saved. The optimization was performed for all signal channels used for spot counting.

Validation of newly optimized classifier

UCBC used for validation of the newly optimized classifier were isolated from umbilical cord blood of three probands (63, 66, and 67). The cells were exposed to 2 Gy γ-irradiation and then the training images displaying γH2AX and 53BP1 levels were captured and recorded by the automated Metafer Slide Scanning System (Version 3.6) (Figure 2). However, their evaluation was done purposely in two ways: 1. the training images were transferred and each cell γH2AX and 53BP1 levels were manually (by eye) counted in the JCountPro program; 2. the automated counting with the newly optimized Metafer classifier. In both cases there was one main condition obeyed – the application of threshold with respect to background where all grey levels less than or equal to the threshold were set to zero.

The following time points of monitoring the γH2AX and 53BP1 foci levels after the irradiation were carried out: 0.5, 1, 2, and 18 hours. For each time point, foci mean values enumeration of the control as well as irradiated samples, at least 500 UCBC were included into the analyses.
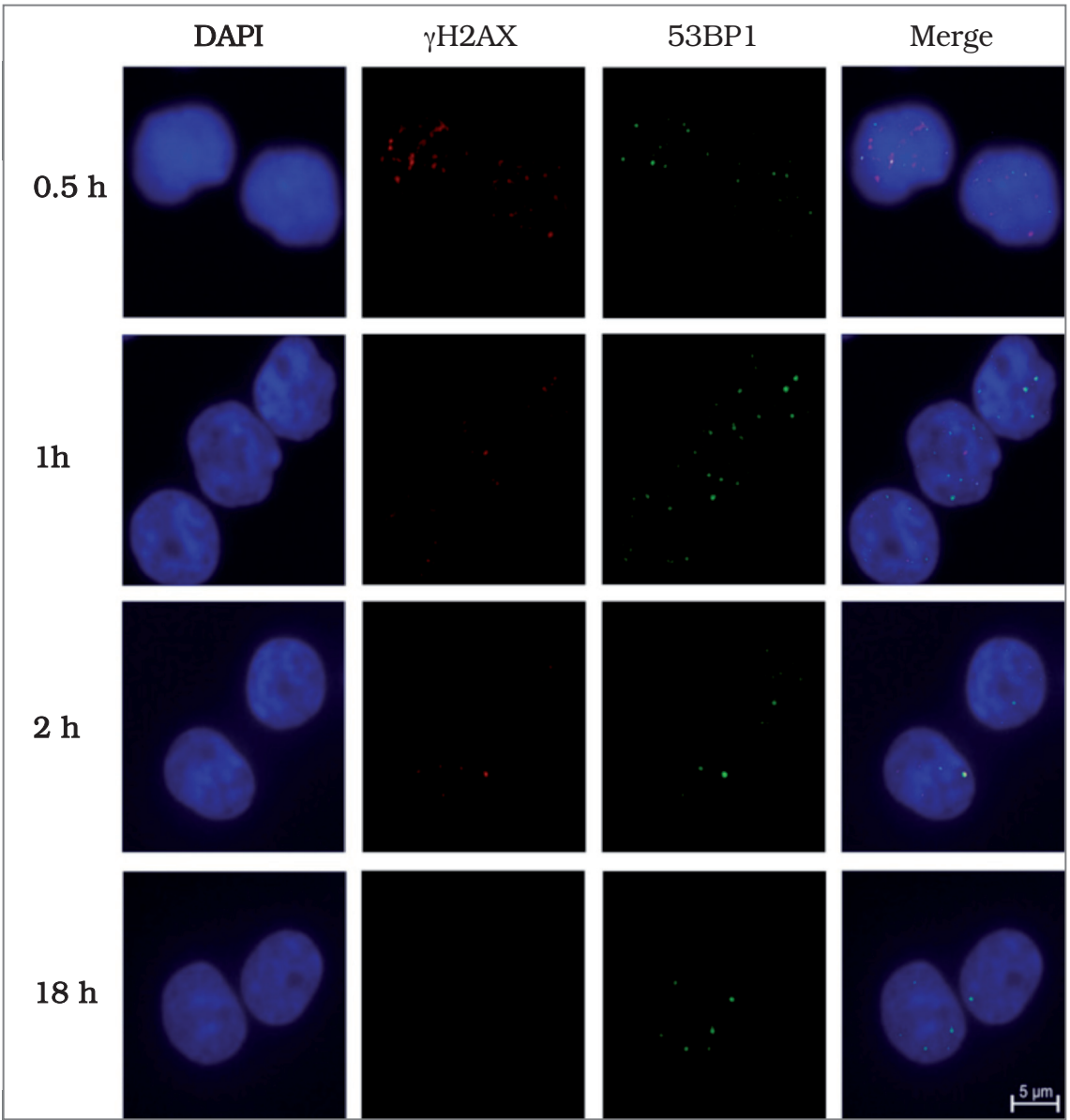
Figure 2. Representative images. The Metafer γH2AX and 53BP1 focus formation in UCBL after γ-irra-diation with a radio-therapeutic dose (2 Gy) at different time points after the exposure.

There was no statistically significant difference found between the Metafer and Image Pro γH2AX and 53BP1 foci mean values enumerations, so we could have considered the new classifier for foci counting as successfully optimized. We also assessed the efficiency of our newly optimized classifier, comparing the mean excess foci levels of γH2AX and 53BP1 (Metafer/JCountPro) in UCBL (Figure 3). The assessed efficiency value equaled to 86.3%, which was a success, considering the fact that the efficiency value of our old classifier fluc-tuated somewhere between 45 – 65%.
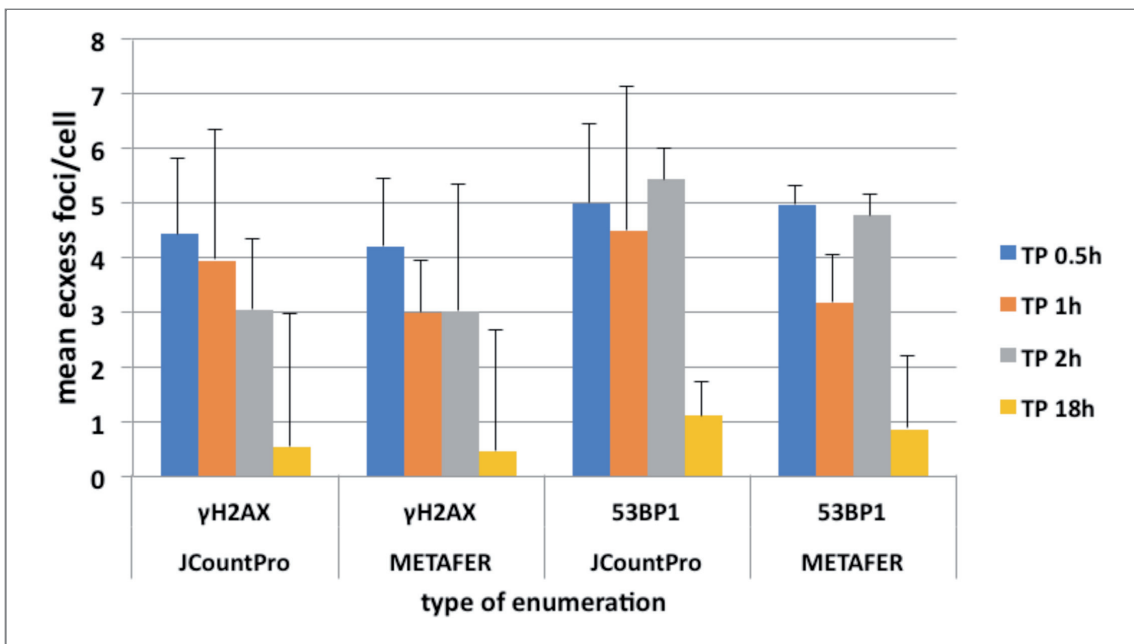
Figure 3. Comparison of the mean excess foci levels of γH2AX and 53BP1. - induced by 2 Gy of γ-irradiation, between the automated newly optimized Metafer system classifier and the manual JCountPro counting in UCBL from three different probands. TP abbreviation stands for time point. The vertical bars represent standard deviations.

DISCUSSION

A real image obtained by using available immunofluorescent staining and confocal microscopy technologies features the presence of the background signal and the variation of the signal in the focus area. The segmentation of such images is usually based on the introduction of the intensity threshold parameter that is present explicitly or implied in majority of focus identification algorithms. The results of the automated focus analysis are highly dependent on the values of the parameters used in a computational approach. Many studies (7, 22, 30) that are based on computational approaches specify the values of these parameters.

According to Qvarnstrom et al. (19) the dependence of the counting results on the chosen parameter values raises the issue of what should be considered as a focus. The results of their study indicate that although the number of automatically counted foci depends on the chosen intensity threshold, the linearity of the dose response is maintained for different threshold values, and therefore it is suggested to use the focus count as a relative measure. This raises the question of how foci counted by an automatic procedure relate to those counted manually and invokes a criticism of automatic focus counting. The simple intensity threshold segmentation also fails to separate two or more adjacent objects (potential foci) if the valley (minimum intensity) between these objects is above the threshold. Another disadvantage of the intensity threshold segmentation is that, due to unavoidable variations between the images in average intensity, individual threshold values need to be applied for various images, and some published algorithms suggest a calculation of individual threshold for each image.

Any computational algorithm designed to identify and count foci operates with a certain number of parameters that need to be specified by the operator. Obviously, algorithms with a smaller number of parameters are preferable since they would be less complicated, easier to learn, and more user friendly. However, there is a certain minimum number of parameters dictated mainly by the quality and complexity of images.

To conclude, the automated focus counting approaches are still evolving with an honest intention to find a reliable, uncomplicated, and at last but not least affordable computational approach.

REFERENCES

1. Bekker-Jensen S, Lukas C, Kitagawa R, Melander F, Kastan MB, Bartek J, Lukas J. 2006. Spatial organization of the mammalian genome surveillance machinery in response to DNA strand breaks. J Cell Biol.173:195 – 206.
2. Rogakou EP, Boon C, Redon C, Bonner WM. 1999. Megabase chromatin domains involved in DNA double-strand breaks in vivo. J Cell Biol. 146:905 – 916.
3. Rothkamm K, Löbrich M. 2003. Evidence for a lack of DNA double-strand break repair in human cells exposed to very low X-ray doses. Proc Natl Acad Sci USA. 100:5057 – 5062.
4. Rothkamm K, Balroop S, Shekhdar J, Fernie P, Goh V. 2007. Leukocyte DNA damage after multi-detector row CT: a quantitative biomarker of low-level radiation exposure. Radiology. 242:244 – 251.
5. Depuydt J, Baert A, Vandersickel V, Thierens H, Vral A. 2013. Relative biological effectiveness of mammography X-rays at the level of DNA and chromosomes in lymphocytes. Int J Radiat Biol. 89:532 – 538.
6. Vandevoorde C, Gomolka M, Roessler U, Samaga D, Lindholm C, Fernet M, Hall J, Pernot E, El-Saghire H, Baatout S, et al. 2015. EPI-CT: in vitro assessment of the applicability of the gamma-H2AX-foci assay as cellular biomarker for exposure in a multicentre study of children in diagnostic radiology. Int J Radiat Biol. 91:653 – 663.
7. Ivashkevich AN, Martin OA, Smith AJ, Redon CE, Bonner WM, Martin RF, Lobachevsky PN. 2011. gammaH2AX foci as a measure of DNA damage: a computational approach to automatic analysis. Mutat Res. 711:49 – 60.
8. Barnard S, Ainsbury E, Al-Hafidh J, Hadjidekova V, Hristova R, Lindholm C, Gil OM, Moquet J, Moreno M, Rößler U. 2014. The first gamma- H2AX biodosimetry intercomparison exercise of the developing European biodosimetry network RENEB. Radiat Protect Dosimetry. ncu259.
9. Lamkowski A, Forcheron F, Agay D, Ahmed EA, Drouet M, Meineke V, Scherthan H. 2014. DNA damage focus analysis in blood samples of minipigs reveals acute partial body irradiation. Plos One. 9:e87458.
10. Viau M, Testard I, Shim G, Morat L, Normil MD, Hempel WM, Sabatier L. 2015. Global quantification of cH2AX as a triage tool for the rapid estimation of received dose in the event of accidental radiation exposure. Mutat Res/Genet Toxicol Environ Mutagenesis. 793:123 – 131.
11. Jakl L, Marková E, Koláriková L, Belyaev I. 2020. Biodosimetry of Low Dose Ionizing Radiation Using DNA Repair Foci in Human Lymphocytes. Genes (Basel). Jan 4; 11(1):58.
12. Horn S, Barnard S, Rothkamm K. 2011. Gamma-H2AX-based dose estimation for whole and partial body radiation exposure. PLoS One. 6:e25113.
13. Wojewodzka M, Sommer S, Kruszewski M, Sikorska K, Lewicki M, Lisowska H, Wegierek-Ciuk A, Kowalska M, Lankoff A. 2015. Defining blood processing parameters for optimal detection of gamma-H2AX foci: a small blood volume method. Radiat Res. 184:95 – 104.
14. Zastko L, Petrovičová P, Račková A, Jakl L, Jakušová V, Marková E, Belyaev I. 2021. DNA damage response and apoptosis induced by hyperthermia in human umbilical cord blood lymphocytes. Toxicology in Vitro. Volume 73. 105127, ISSN 0887-2333.
15. Markova E, Schultz N, Belyaev IY. 2007. Kinetics and dose-response of residual 53BP1/gamma-H2AX foci: co-localization, relationship with DSB repair and clonogenic survival. Int J Radiat Biol. 83:319 – 329.

16. Groesser T, Fontenay GV, Han J, Chang H, Pluth J, Parvin B. 2015. Quantification of the dynamics of DNA repair to ionizing radiation via colocalization of 53BP1 and gamma H2AX. In: Bhanu B, Talbot P, editors. Video bioinformatics: from live imaging to knowledge: Computational Biology Series, v. 22: Dordrecht: Springer. p. 253 – 263.
17. Vandevoorde C, Gomolka M, Roessler U, Samaga D, Lindholm C, Fernet M, Hall J, Pernot E, El-Saghire H, Baatout S, et al. 2015. EPI-CT: in vitro assessment of the applicability of the gamma-H2AX-foci assay as cellular biomarker for exposure in a multicentre study of children in diagnostic radiology. Int J Radiat Biol. 91:653 – 663.
18. Zastko L, Račková A, Petrovičová P, Durdík M, Míšek J, Marková E, Belyaev I. 2021. Evaluation of Calyculin A Effect on γH2AX/53BP1 Focus Formation and Apoptosis in Human Umbilical Cord Blood Lymphocytes. Int J Mol Sci. 22(11):5470.
19. Qvarnstrom OF, Simonsson M, Johansson KA, Nyman J, Turesson I. 2004. DNA double strand break quantification in skin biopsies. Radiother Oncol. 72:311 – 317.
20. Bocker W, Iliakis G. 2006. Computational methods for analysis of foci: validation for radiation-induced gamma-H2AX foci in human cells. Radiat Res. 165:113 – 124.
21. Barber P, Locke R, Pierce G, Rothkamm K, Vojnovic B. 2007. Gamma- H2AX foci counting: image processing and control software for highcontent screening: Biomedical Optics (BiOS) 2007:64411M–64411M-10.
22. Hou Y-N, Lavaf A, Huang D, Peters S, Huq R, Friedrich V, Rosenstein BS, Kao J. 2009. Development of an automated c-H2AX immunocytochemistry assay. Radiat Res. 171:360 – 367.
23. Roch-Lefevre S, Mandina T, Voisin P, Gaetan G, Mesa JE, Valente M, Bonnesoeur P, Garcia O, Voisin P, Roy L. 2010. Quantification of gamma-H2AX foci in human lymphocytes: a method for biological dosimetry after ionizing radiation exposure. Radiat Res. 174:185 – 194.
24. Turner HC, Sharma P, Perrier JR, Bertucci A, Smilenov L, Johnson G, Taveras M, Brenner DJ, Garty G. 2014. The RABiT: high-throughput technology for assessing global DSB repair. Radiat Environ Biophys. 53:265 – 272.
25. Kosik P, Durdik M, Jakl L, Skorvaga M, Markova E, Vesela G, Vokalova L, Kolariková L, Horvathova E, Kozics K, Belyaev I. 2020. DNA damage response and preleukemic fusion genes induced by ionizing radiation in umbilical cord blood hematopoietic stem cells. Sci Rep. 10. 13722.
26. Misek J, Laukova T, Kohan M, Veternik M, Jakusova V, Jakus J. 2018.Measurement of Low-level radiofrequency electromagnetic fields in the human environment. Acta Medica Martiniana. 18(2): 27 – 33.
27. Sladicekova K, Bereta M, Misek J, Parizek D, Jakus J. 2021. Biological effects of a low-frequency electromagnetic field on yeast cells of the genus Saccharomyces Cerevisiae. Acta Medica Martiniana. 21(2): 34 – 41.
28. Jakl L, Lobachevsky P, Vokálová L, Durdík M, Marková E, Belyaev I. 2016. Validation of JCountPro software for efficient assessment of ionizing radiation-induced foci in human lymphocytes. Int J Radiat Biol. 92(12):766 – 773.
29. Vasilyev SA, Kubes M, Markova E, Belyaev I. 2013. DNA damage response in CD133 + stem/progenitor cells from umbilical cord blood: low level of endogenous foci and high recruitment of 53BP1. Int J Radiat Biol. 89:301 – 309.
30. Cai Z, Vallis KA, Reilly RM. 2009. Computational analysis of the number, area and density of gamma-H2AX foci in breast cancer cells exposed to (111) In-DTPAhEGF or gamma-rays using Image-J software. Int J Radiat Biol. 85:262 – 271.

ASSOCIATION OF GENETIC VARIABILITY IN SELECTED GENES WITH PLATELET HYPERAGGREGABILITY AND ARTERIAL THROMBOSIS

Brunclikova Monika[1], Ivankova Jela[1], Skerenova Maria[2], Simurda Tomas[1], Stanciakova Lucia[1], Skornova Ingrid[1], Sterankova Miroslava[1], Zolkova Jana[1], Dobrotova Miroslava[1], Holly Pavol[1], Kubisz Peter[1], Stasko Jan[1]

[1]National Centre of Hemostasis and Thrombosis, Department of Hematology and Transfusiology, Comenius University in Bratislava, Jessenius Faculty of Medicine in Martin and University Hospital in Martin, Slovakia
[2]Biomedical Centre Martin, Comenius University in Bratislava, Jessenius Faculty of Medicine in Martin, Slovakia

A b s t r a c t

Introduction: Inherited platelet hyperaggregability, so called "Sticky platelet syndrome" (SPS), is a prothrombotic platelet disorder. The syndrome contributes more often to arterial than venous thrombosis. The most common localization of arterial occlusion involves cerebral or coronary arteries. However, SPS may also lead to thrombosis in the atypical sites of the circulation. This qualitative platelet alteration causes platelet hyperaggregability after a very low concentration of platelet inducers – adenosine diphosphate (ADP) and/or epinephrine (EPI). The precise genetic background of the syndrome has not been defined. In the present study we aimed to determine the association between selected single nucleotide polymorphisms (SNPs) within genes for platelet endothelial aggregation receptor 1 (PEAR1) and murine retrovirus integration site 1 (MRVI1) and the risk for arterial thrombosis in patients with SPS. The products of these selected genes play an important role in platelet aggregation.

Patients and methods: We examined 69 patients with SPS and a history of arterial thrombosis and 69 healthy blood donors who served as controls. SPS was confirmed by a light transmission aggregometry (LTA) according to the method and criteria described by Mammen and Bick. We assessed two SNPs within PEAR1 gene (rs12041331, rs1256888) and two SNPs within MRVI1 gene (rs1874445, rs7940646).

Results: Selected PEAR1 and MRVI1 polymorphisms seem not to be a risk factor for the development of SPS as the syndrome with an arterial thrombosis phenotype. However, in the subgroup of SPS1 patients there was found a decreased frequency of the minor A allele of SNP rs12041331 in PEAR1 gene (borderline p value, p=0.061) that can be hypothesized as protective against arterial thrombosis. In the same SPS1 subgroup the haplotype TA in PEAR1 gene also showed a decreased frequency with a borderline insignificance (p=0.056). We can theorize also about its protective role in SPS1 patients. We did not confirm the protective effect of polymorphism (T/T of rs 12566888) in PEAR1 against arterial thrombosis in SPS patients and SPS subgroups.

Conclusion: Our results support the idea that examined genetic variability of the selected SNPs in PEAR1 and MRVI1 genes is not associated with platelet hyperaggregability manifested as arterial thrombosis. The possible protective role of the minor A allele of SNP rs12041331 as well as a role of haplotype TA in PEAR1 gene related to the arterial thrombosis found in the subgroup of SPS1 patients needs to be verified in further research.

Key Words: Sticky platelet syndrome, platelet hyperaggregability, arterial thrombosis

Corresponding author: Brunclikova Monika, MD; simkovamonika@gmail.com; phone: +421-43-4203232, Fax: +421-43-4132061

INTRODUCTION

While the physiological function of platelets is to support arrest of bleeding, to contribute to wound healing, to restore vessel wall integrity and host defence, platelets can form occlusive thrombi. Their dysfunction is one of the crucial causes of arterial thrombosis which leads to the development of acute ischemic syndromes (1). Platelet hyperaggregability triggered by low concentrations of platelet agonists adenosinediphosphate (ADP) and/or epinephrine (EPI), referred to as sticky platelet syndrome (SPS), has been identified in approximately 21% of unexplained arterial thrombotic events, regarded to be the most common thrombophilia in arterial thrombosis (2 – 4). Furthermore, this syndrome has been described also in patients with venous thrombosis and in women with recurrent fetal loss without a personal history of thrombosis (5 – 7). SPS is possibly the leading cause of thrombotic occlusions in the atypical parts of the circulation (8). Clinical symptoms of SPS commonly occur in stressful situations and can develop even on an adequate dose of oral anticoagulant therapy (9). The first thrombosis usually occurs in patients younger than 40 years and with or without acquired risk factors (10).

SPS is diagnosed by aggregometry according to the method of Mammen and Bick with the use of three different concentrations of ADP and EPI. Robust aggregation to a low concentration of listed inductors establishes a true hyperreactive platelet phenotype (11). Aggregation in response to other agonists (ristocetin, arachidonic acid, thrombin, collagen) remains normal (12). Depending on the results of this examination, three types of SPS are defined: hyperaggregation after both ADP and EPI is classified as type I, increased aggregation induced only by EPI is type II, and type III – an increased aggregation induced by ADP **(Figure1)** (13 – 15).
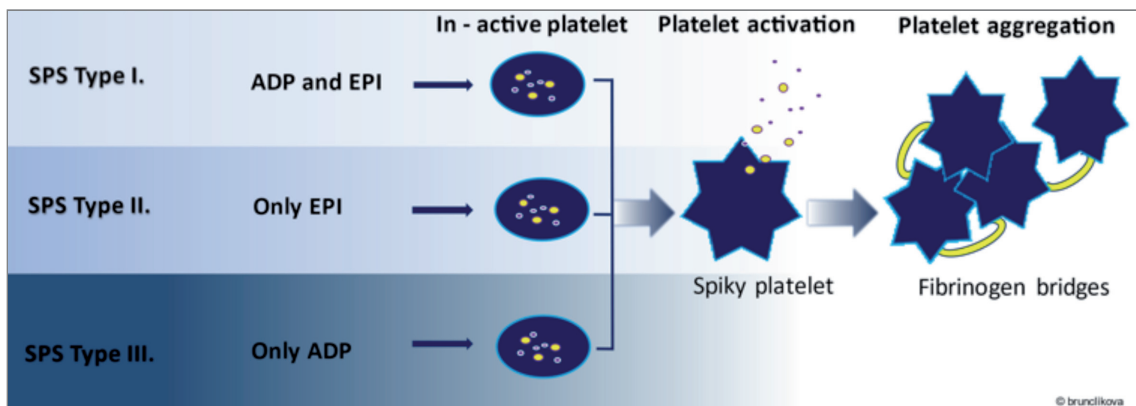
Fig. 1. Laboratory classification of sticky platelet syndrome (original figure)

One of the distinctive features of SPS is a familial occurrence of the disease and the affection of both genders (10). SPS shows an autosomal pattern of inheritance (9). The etiopathogenesis of the syndrome has not been fully understood (16, 17). It has been suggested that the defects of the platelet membrane glycoproteins (GP) can be responsible for the disorder (15). The second mechanism underlying the hyperreactivity to different types of platelet stimulation may affect intracellular signalling pathways (12). However, although several studies have described some possible mechanisms involved in its background, the exact genetic cause has not been identified yet. In a genome-wide meta-analysis, 2,5 million SNPs with a platelet aggregation response to some agonists (also to ADP, EPI) were tested in European ancestry cohorts and identified 7 loci with platelet aggregation. Based on this study we selected some SNPs in two genes - PEAR1 and MRVI1 (18).

Platelet Endothelial Aggregation Receptor (PEAR1)

PEAR1 is a receptor of the Epidermal Growth Factor (EGF) family which is expressed on the surface of megakaryocytes, platelets, and endothelial cells. PEAR1 is also present on inactive platelets as well as in their α granules. After a platelet stimulation, PEAR1 is secreted from α granules and phosphorylated as a coagulation receptor. Its expression at the membrane surface is thereby implicated in the regulation of hemostasis. This receptor has tyrosine kinase (RTK) property, causing an interaction between platelets via the Emilin Family Domain (EMI domain) in its extracellular part and triggering PI3K/AKT/PTEN signalling. Afterward, by triggering of PI3K/AKT/PTEN pathway, GPIIb/IIIa, which is a crucial factor in aggregation, is activated. Thus, phosphatidylinositol 3-kinase (PI3K) complex activates and stimulates aggregation (19).

PEAR1 gene has 23 exons and 22 introns, some polymorphisms of this gene impair platelet function and increase platelet aggregation. Some polymorphisms were involved in the process of heart disease (19). In addition, Sokol et al. described a possible protective effect of polymorphism (T/T of rs 12566888) within PEAR1 against fetal loss in women with SPS (14).

Murine retrovirus integration site 1 (MRVI1, IRAG)

Nitric oxide (NO) is a potent vasodilatator, a platelet inhibitor, and an elevator of cellular cGMP levels. Functionally, cGMP elevation inhibits agonist-induced integrin activation, granule secretion, TXA2 synthesis/release, and cytoskeleton rearrangement in platelets. cGMP and cAMP levels regulate cGMP and cAMP- dependent protein kinase A (PKA) and G (PKG) which phosphorylate multiple substrates involved in platelet inhibition. MRVI1 by PKG inhibits agonist induced Ca^{2+} mobilization and platelet activation (20). MRVI1 homolog which showed both EPI and ADP induced associations has a prior evidence of function in platelet aggregation. In mice, MRVI1 has a direct role in the inhibition of platelet aggregation and in vivo thrombosis (9).

The aim of the presented study was to evaluate the genetic variability of selected genes (MRVI1, PEAR1) both in the patients with the SPS manifested with arterial thrombosis and in

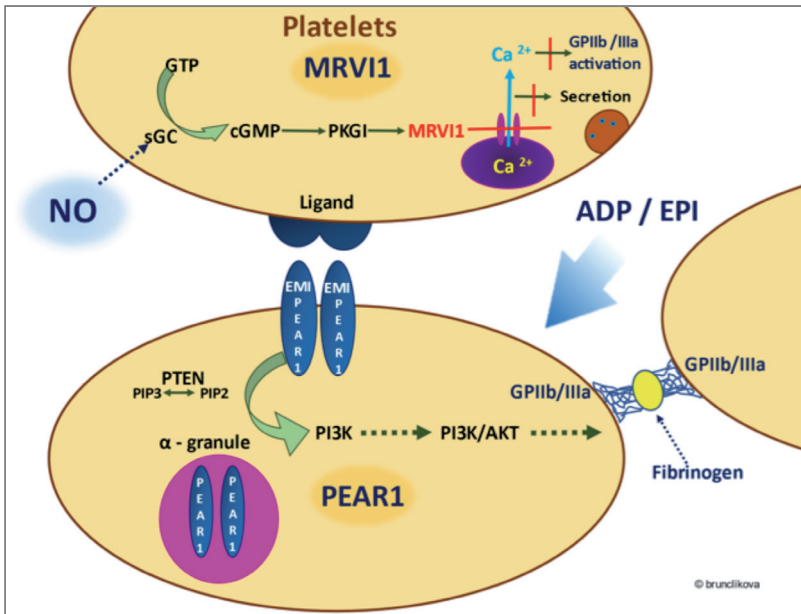**Figure 2.** Platelets and function of PEAR1, MRVI1

PEAR1: PEAR1 secretes from platelet alpha granules and emerges to the surface, then bounds to one of its ligands (EMI Domain), triggers a PI3K/AKT/PTEN signalling pathway. This non – Syk pathway increases the expression of GPIIb/IIIa.

MRVI1 – IRAG: Activation of MRVI1 results in a reduced calcium release from intracellular stores (19, 21).

the control group, carry out association analysis of the genetic changes with the syndrome and its type, and thus identify a relationship between the selected regions of the genes and SPS with arterial thrombosis. **Figure 2** shows the function of PEAR1 and MRVI1 and their mechanisms of action.

MATERIAL AND METHODS

Study population and Inclusion/Exclusion Criteria

The study was approved by the local Ethical Committee of the Jessenius Faculty of Medicine in Martin (Number EK129/2019). The informed consent in accordance with the Declaration of Helsinki was obtained from each participant. In case of a person less than 18 years old the signed consent from parents or guardians was received prior to their involvement in the study.

The patients were initially examined and tested at the Department of Hematology and Transfusiology in Martin University Hospital. They were referred to the hematology by their specialists (neurologist, cardiologist, and other physicians) in order to undergo a thrombophilia screening as a part of differential diagnosis of a thrombotic event. The patients with verified arterial thrombotic events (IS, MI, and arterial thrombosis at other sites) and confirmed SPS according to the criteria of Mammen and Bick (see below) were subsequently asked to participate in the study and undergo a genetic testing. Thus, all participants fulfilled the inclusion criteria: at least one episode of an arterial thrombotic event up to the age of 45, confirmed SPS according to the Mammen and Bick criteria, and voluntary participation in the study and signed informed consent. We focused on young people in order to reduce a number of other risk factors that could contribute to the development of atherosclerosis or arterial thrombotic events. The occurrence of other thrombotic episode, e. g. venous thrombosis or miscarriage, the presence of other thrombophilic state, and smoking, were not considered as a reason for the exclusion of the patients. The exclusion criteria included: insufficiently verified arterial thrombosis, active or chronic disease or active cancer, current pregnancy, age above the specified age limit, liver or kidney failure, and a lack of the informed consent. Altogether 138 participants were enrolled in the study. 69 patients with SPS and arterial thrombosis in personal history and 69 randomly chosen age – matched healthy blood donors. All control individuals – blood donors, were Caucasians of European origin with a negative family and personal history and a normal platelet aggregability after a stimulation by an ADP and/or EPI agonist according to the method by Mammen and Bick.

All blood samples in both study groups were taken outside the menstrual period, active haemorrhage, or acute infection. No blood sample was taken during an acute phase of thrombosis. The light transmission aggregometry (LTA) was performed in the patients without antiplatelet therapy (the discontinuation of ADP inhibitors, ASA, nonsteroidal anti-inflammatory, direct oral anticoagulants, or other drugs with possible effect on platelets for at least 7 days before testing).

Table 1 summarized basic characteristics of SPS patients and control group.

Table 1. Characteristics of SPS patients and the control group

Characteristics	Patients with SPS	Controls
Number of patients	69	69
Age (mean ± SD)	34.7 ± 9.8	31.7 ± 7.6
Male/women	26/43	40/29
SPS type I	17 (25%)	–
SPS type II	52 (75%)	–

SPS examination by the Light transmission aggregometry

The venous blood drawn from antecubital vein was collected into the tubes of 3.2% buffered sodium citrate. The anticoagulant – blood ratio was 1:10. The samples were processed and analysed within 2 hours after their collection. The aggregometry testing was performed with platelet rich plasma using AggRAM aggregometer, Helena Laboratories, according to the criteria by Mammen and Bick. Each sample was tested with 3 low concentrations of platelets agonists – ADP (2.34 µmol/L, 1.17 µmol/l, 0.58 µmol/L) and EPI (11 µmol/L, 1.1 µmol/L, 0.55 µmol/L). The normal aggregation ranges are depicted in **Table 2.** The diagnosis of SPS was confirmed with hyperaggregability after two or more concentrations of either reagent or one alternatively more concentrations of both reagents and a history of a thrombotic event.

Table 2 Normal aggregation ranges in our laboratory

Aggregation with EPI	Concentration EPI	Reference values
	11 µmol/l	60 – 90 %
	1.1 µmol/l	11 – 30 %
	0.55 µmol/l	8 – 15 %
Aggregation with ADP	Concentration ADP	
	2.3 µmol/l	20 – 60 %
	1.2 µmol/l	11 – 23 %
	0.6 µmol/l	3 – 10 %

PEAR1, MRVI1 genes analysis

The peripheral venous blood drawn from the antecubital vein was collected into tubes containing EDTA. The blood was processed within 2 hours of collection and stored, if necessary, at - 20°C. Genomic DNA was obtained from leukocytes by SiMax Genomic DNA Extraction kit (SBS Genetech Co, Ltd, Beijing, China) according to the manufacturer´s instructions. The high resolution melting (HRM) analysis was performed with the designed primers on LightCycler 480II (Roche Diagnostics, Germany) for genotyping. We selected the following SNPs for the genetic analysis: 2 SNPs (rs12041331, rs1256888) within PEAR1 and 2 SNPs (rs1874445, rs7940646) within MRVI1. The sequenced SNPs and their basic characteristics are summarized in **Table 3.**

Table 3. Characteristics of the Selected SNPs

Gene	SNP Number	SNP Sequence	Major/Minor Alelle	Chromosome	Position Within Gene
PEAR1	rs12041331	CTTCC[G/A]TCACC	G/A	1	Intronic
PEAR1	rs1256888	TCCAG[G/T]ATAGG	G/T	1	Intronic
MRVI1	rs1874445	GTTTT[G/A]ACTCA	G/A	11	Intronic
MRVI1	rs7940646	GACAG[G/A]CCCAC	G/A	11	Intronic

Statistical Evaluation

Haplotype and single marker association analysis was performed with software Plink 1.9 (www.cog-genomics.org/plink/1.9/). The Fischer exact test was used to estimate a significance of deviation from Hardy – Weinberg equilibrium and to execute the basic allelic genotypic (recessive and dominant model) association. Statistically significant were considered P – values less than 0.5%. To assess risk were used odds ratio (OR) with 95% interval.

RESULTS

Overall, 138 patients were examined, 69 patients with SPS and arterial thrombosis in personal history up to the age of 45 and 69 healthy control participants (blood donors) with an average age 34.7± 9.8 and 31.7 ± 7.6, respectively. 17 patients (25%) were confirmed as SPS type I, 52 patients (75%) had SPS type II according to Mammen and Bick criteria.

In sum, we examined 4 SNPs. All polymorphisms were localized in intronic regions (2 SNPs within PEAR1 gene: rs12041331, rs1256888, and 2 SNPs within MRVI1 gene: rs1874445, rs7940646). We tested the allelic association in SPS patients with an arterial thrombosis in history. The minor allele A of SNP within the PEAR1 gene (rs 12401331) had a lower incidence compared with the control subjects but did not reach a significant value (frequency in SPS patients 0.043, compared to healthy controls with frequency 0.087, OR 0.477, 95% CI 0.174 – 1.310). We did not observe any statistically significant higher or lower occurrence of any rs variants in the patients with SPS and arterial thrombosis compared to the healthy controls. The frequency of all tested alleles and genotypes was comparable between both the control and the SPS patients' group. Our results are summarized in **Table 4** and **Table 5**.

We tried also to assess the frequency of subgroup analysis by type of SPS in these 4 SNPs. We found a decreased frequency of the minor allele A of SNP rs12041331in PEAR1 gene in the subgroup of SPS1 patients compared to the healthy controls, which was of a borderline insignificance (p=0.061) **(Table 4)**. Similarly, there was a decreased frequency of haplotype TA in PEAR1 gene in the SPS1 subgroup compared to the controls, again with a borderline insignificance (p=0.056) **(Table 5)**. The frequency of other tested alleles and genotypes in the SPS subgroups was comparable between both the control and the SPS patients' subgroup.

Table 4. Frequency of examined alleles within PEAR1, MRVI1 in patients with SPS and arterial thrombosis compared to the control group

Gene	SNPs	Minor allele	Frequency	Frequency	Fisher's Exact P allelic association	OR Minor allele	95% CI	Fisher's Exact P genotypic association	Exact Armitage P genotypic additive association
			All SPS cases	**Controls**					
PEAR1	rs12566888	T	0.051	0.087	0.342	0.561	0.214-1.471	0.323	0.217
PEAR1	rs12041331	A	0.043	0.087	0.222	0.477	0.174-1.310	0.206	0.129
MRVI1	rs7940646	A	0.434	0.355	0.218	1.397	0.861-2.268	0.386	0.152
MRVI1	rs1874445	A	0.514	0.442	0.278	1.338	0.833-2.148	0.438	0.188
			SPS1 cases	**Controls**					
PEAR1	rs12566888	T	0.025	0.087	0.303	0.269	0.034-2.137	0.283	0.167
PEAR1	**rs12041331**	A	0.000	0.087	0.071	0.000	-	**0.061**	0.045
MRVI1	rs7940646	A	0.450	0.355	0.354	1.486	0.728-3.034	0.459	0.256
MRVI1	rs1874445	A	0.550	0.442	0.281	1.543	0.760-3.131	0.417	0.191
			SPS2 cases	**Controls**					
PEAR1	rs12566888	T	0.063	0.087	0.621	0.700	0.253-1.935	0.605	0.471
PEAR1	rs12041331	A	0.063	0.087	0.621	0.700	0.253-1.935	0.605	0.471
MRVI1	rs7940646	A	0.427	0.355	0.278	1.354	0.794-2.390	0.495	0.235
MRVI1	rs1874445	A	0.500	0.442	0.425	1.262	0.749-2.128	0.661	0.343

* SNPs – single nucleotide polymorphisms, SPS – sticky platelet syndrome, CI – confidence interval

Table 5. Haplotype frequencies within PEAR1, MRVI1 in SPS patients with arterial thrombosis compared to the controls

		F SPS	F Controls	P Value	OR	95% CI
All SPS						
PEAR1	GG	0.963	0.913	0.088	2.533	0.868 - 7.396
	TA	0.037	0.087	0.088	0.394	0.135-1.152
MRV1	GG	0.478	0.558	0.185	0.726	0.452-1.166
	AA	0.427	0.355	0.226	1.357	0.351-2.203
	AG	0.096	0.087	0.804	1.092	0.480-2.486
SPS2						
PEAR1	GG	0.947	0.913	0.333	1.733	0.590-5.091
	TA	0.053	0.087	0.333	0.577	0.196-1.695
MRV1	GG	0.495	0.558	0.342	0.792	0.470-1.336
	AA	0.421	0.355	0.308	1.297	0.760-2.215
	AG	0.084	0.087	0.941	0.955	0.375-2.432
SPS1						
PEAR1	GG	1.000	0.913	0.056	8.004	0.464-138.207
	TA	0.000	0.087	**0.056**	0.125	0.007-2.157
MRV1	GG	0.436	0.558	0.177	0.612	0.299-1.253
	AA	0.436	0.355	0.357	1.404	0.681-2.891
	AG	0.128	0.087	0.440	1.544	0.509-4.685

*SPS – sticky platelet syndrome, F – frequency, OR – odds ratio, CI – confidence interval

DISCUSSION

Ischemic stroke, myocardial infarction, and others forms of arterial thrombosis are leading causes of death and disability worldwide, usually result from a rupture of the atherosclerotic plaque, leading to an arterial thrombus formation followed by a distal tissue infarction (22). However, in the clinical practice we also encounter patients in whom the formation of a thrombus in the arterial system is not caused by atherosclerosis but by other causes. Platelets are crucial for the development of such thrombi (23). SPS is one of the major factors which is associated with an increased risk for arterial thrombosis and less often with venous thrombosis. Over the past three decades, a substantial progress has been made in the understanding of this disorder, the role of hyperaggregable

platelets in thrombus formation, the diagnostic and treatment procedures. However, there are still unanswered questions surrounding the genetic background and SPS inheritance pattern.

The main purpose of our work and research was to examine the association between the selected SNPs and the risk for arterial thrombosis in the patients with SPS. The products of the selected genes play a crucial role in the platelet aggregation. PEAR1 gene and its expression at the membrane surface are also implicated in the regulation of hemostasis. This receptor has a tyrosine kinase property and causes an interaction between the platelets and the platelet aggregation. Sokol et al described a possible protective effect of polymorphism (T/T of rs 12566888) within PEAR1 gene against fetal loss in women with SPS (14). The last gene product, MRVI1 inhibits agonist induced Ca^{2+} mobilization and platelet activation. In mice, MRVI1 has a direct role in the inhibition of platelet aggregation and in vivo thrombosis.

In this study, we did not find any significantly higher occurrence of the selected SNPs and the chosen haplotype in SPS patients with a history of arterial thrombosis compared to healthy individuals. These polymorphisms seem not to be a risk factor for the development of SPS with an arterial thrombosis phenotype. We also did not confirm the protective effect of polymorphism (T/T of rs 12566888) within PEAR1 against arterial thrombosis compared to the described study in women with fetal loss and SPS (14).

However, in the subgroup of SPS1 patients there was found a decreased frequency of the minor A allele of SNP rs12041331 in PEAR1 gene (borderline p value, p=0.061). We can hypothesize about a possible protective effect of the minor A allele (rs12041331) against arterial thrombosis in the SPS1 subgroup. In the same SPS1 subgroup we verified a decrease frequency of the haplotype TA in PEAR1 gene, again with a borderline insignificance (p=0.056). Similarly, as in the case of allele A (rs12041331) we can theorize about the protective role of haplotype TA related to the thrombosis in the SPS1 subgroup of patients.

However, our study had several limitations, including the number of patients with SPS and arterial thrombosis. The target population of our analysis consisted of patients with hyperaggregable platelets who developed the arterial thrombosis at a younger age than the general population, which draws the attention rather to genetic than to acquired risk factors. The risk and incidence of arterial thrombosis is strongly dependent on age, increases with age and aging, accompanied factors such as obesity, blood pressure, serum cholesterol, and diabetes. Due to the age limit, the number of patients in the cohort was relatively small. Another limitation was a possible impact in the patients' selection from the Slovak population. In different races and populations the same disease state may be achieved by different genotypes affecting different mediating mechanisms. There are differences between and among populations and races in SNPs and haplotype frequencies, different mutations and reproduction of gene variants, gene flows between populations through migration, and similar matters. Large multicentric population – based studies focusing on the impact of PEAR1 and MRVI1 gene variability on the arterial thrombosis risk in SPS patients are needed to better understand genetic and molecular biology of the syndrome. Further research should shed light on the development of SPS and may help to predict arterial thrombotic events in these patients.

REFERENCES

1. Scharf R.E. Acquired Disorders of Platelet Function. Platelets 2019; 905 – 906. DOI: 10.1016/B.978-0-12-813456-6.00049-7

2. Sokol J, Skerenova M, Jedinakova Z, Simurda T, Skornova I, Stasko J, Kubisz P. Progress in the Understanding of Sticky Platelet Syndrome. Semin Thromb Hemost. 2016; DOI: 10.1055/s - 0036-1584352

3. Kubisz P, Stanciakova L, Stasko J, Dobrotova M, Skerenova M, Ivankova J, Holly P. Sticky platelet syndrome: an important cause of life–threatening thrombotic complications. Expert Rev Hematol. 2016; 9:21 -35. DOI: 10.1586/17474086.2016.1121095

4. Garcia – Navarette YI, Vallejo – Villalobos MF, Olivares – Gazca JM, Cantero – Fortiz Y, León – Pena A, Olivares – Gazca JC, Murrieta – Alvarez I, Ruiz – Delgado G, Ruiz – Arguelles G. Primary thrombophilia XV: antithrombotic treatment of sticky platelet syndrome worldwide. Ann Blood 2019; 4: 15. DOI: 10.21037/aob.2019.06.05

5. Skerenova M, Sokol J, Biringer K, Ivankova J, Stasko J, Kubisz P, Lasabova Z. GP6 Haplotype of Missense Variants is Associated with Sticky Platelet Syndrome Manifested by Fetal Loss. Clinical and Applied Thrombosis/Hemostasis 2018; 24(1):63 – 69. DOI:10.1177/1076029616685428.

6. Vallejo – Villalobos MF, Gomez – Cruz GB, Cantero – Fortiz Y, Olivares – Gazca JC, Olivares – Gazca M, Murrieta – Alvarez I, Reyes- Nunes V, Ruiz – Arguelles GJ. Primary Thrombophilia XVI: Worldwide Identification of Sticky Platelet Syndrome. Semin Thromb Hemost 2019; 45: 423 – 428. DOI: 10.1055/s-0039-1688498

7. Ruiz – Delgado G, Cantero – Fortiz Y, Mendez – Huerta MA, Leon – Gonzales M, Nunez – Cortes A, Leno – Pena A, Olivares – Gazca JC, Ruiz – Arguelles GJ. Primary Thrombophilia in Mexico XII: Miscarriages Are More Frequent in People with Sticky Platelet Syndrome. Turk J Hematol 2017; 34: 239 – 243. DOI: 10.4274/thj.2016.0411

8. Stanciakova L, Skerenova M, Holly P, Dobrotova M, Ivankova J, Stasko J, Kubisz P. Genetic origin of the sticky platelet syndrome. Rev Hematol Mex. 2016, 17 (2): 139 – 143

9. Sokol J, Skerenova M, Ivankova J, Simurda T, Stasko J. Association of Genetic Variability in Selected genes in Patients with Deep Vein Thrombosis and Platelet Hyperaggregability. Clinical and Applied Thrombosis/Hemostasis 2018; 24(7):1027-1032. DOI: 10.1177/1076029618779136

10. Kubisz P, Ruiz – Arguelles GJ, Stasko J, Holly P, Ruiz – Delgado GJ. Sticky platelet syndrome: history and future perspectives. Semin Thromb Hemost. 2014; 40: 526 – 34. DOI: 10.1055/s- 0034-1381235

11. Kubisz P, Bartosova L, Ivankova J, Holly P, Stasko J, Skerenova M, Pullman R. Is Gas6 protein associated with sticky platelet syndrome? Clin Appl Thromb Hemost 2010; 16(6):701 -704

12. Cesarman – Maus G, Villa R, Kubisz P, Gonzales – Ramirez M, Ruiz – Delgado G, Ruiz – Arguelles GJ. The Sticky Platelet Syndrome. Rev Hematol Mex 2013; 14: 149 – 153.

13. Azamar-Solis B, Cantero – Fortiz Y, Olivares – Gazca JC, Olivares – gazca JM, Goméz – Cruz GB, Murrieta – Alvarez I, Ruiz Delgado GJ, Ruiz – Arguelles GJ. Primary Thrombophilia in Mexico XII: Localization of Thrombotic Events in Mexican Mestizos With the Sticky Platelet Syndrome. Clinical and Applied Thrombosis/Hemostasis 2019; 25: 1-4. DOI: 10.1177/1076029619841700.

14. Sokol J, Biringer K, Skerenova M, Stasko J, Kubisz P, Danko J. Different models of inheritance in selected genes in patient with sticky platelet syndrome and fetal loss. Semin Thromb Hemost 2015; 41:330-335

15. Stasko J, Holly P, Kubisz P. A new decade awaits sticky platelet syndrome: where are we now, how do we manage and what are the complications? Exp Rev Hematol 2022; 15(1):53-63. https://doi.org/10.1080/17474086.2022.2030217

16. Kubisz P, Holly P, Stasko J. Sticky Platelet syndrome: 35 Years of Growing Evidence. Seminars in Thrombosis and Hemostasis 2019; 45(1): 61-68. DOI https://doi.org/10.1055/s-0038-1676581.

17. De Cima S, Zamora – Ortiz G, Hernandez _ Reyes J, Vargas – Espinosa J, Garcia – Chavez J, Rosales – Padron J, Ruiz – Delgado G, Ruiz – Arguelles A, Ruiz – Arguelles GJ. Primary Thrombophilia in Mexico X: A Prospective Study of the treatment of the Sticky Platelet Syndrome. Clinical and Applied Thrombosis/Hemostasis 2015; 21(1): 91 – 95. DOI: 10.1177/1076029613501543

18. Kubisz P, Ivankova J, Skerenova M, Stasko J, Holly P. The prevalence of the glycoprotein VI polymorphisms in patients with sticky platelet syndrome and ischemic stroke. Hematology. 2012,17;355 / 362. DOI: 10.1179/1024533212Z.000000000142

19. Ansari N, Najafi S, Shahrabi S, Saki N. PEAR1 polymorphisms as a prognostic factor in hemostasis and cardiovascular disease. Journal of Thrombosis and Thrombolysis; 2020. DOI: 10.1007/s11239-020-02149

20. Makhoul S, Walter E, Page O, Walter U, Sickman A, Gambaryan S, Smolenski A, Zahedi R. P, Jurk K. Effects of the NO/soluble guanylate cyclase/cGMP system on the functions of human platelets. Nitric Oxide 2018; 76: 71 – 80. DOI: 10.1016/j.niox.2018.03.008.

21. Loyau S, Dumont B, Ollivier V, Boulaftali Y, Feldman L, Ajzenberg N, Jandrot-Perrus M. Platelet Glycoprotein VI Dimerization, and Active Process Inducing Receptor Competence, Is an Indicator of Platelet reactivity. Arteriosclerosis, Thrombosis and Vascular Biology. 2012; 32(3):778 – 785. DOI: 10.116/ATVBAHA.111.241067.

22. Induruwa I, Moroi M, Bonna A, Malcor D, Howes M, Warburton E.A, Farndale R.W, Jung M. Platelet collagen receptor Glycoprotein VI – dimer recognizes fibrinogen and fibrin through their D – domains, contributing to platelet adhesion and activation during thrombus formation. Journal of Thrombosis and Haemostasis 2017; 16: 389 – 404. DOI: 10.1111/jht.13919

23. Kim D, Bresette Ch, Liu Z, Ku D.N. Occlusive thrombosis in arteries. APL Boeing 2019; 3. DOI:10:1063/1.5115554.

NURSING STUDENTS´ PERCEPTION OF PATIENT SAFETY CULTURE DURING THE COVID-19 PANDEMIC – RESULTS OF A PILOT STUDY

KALANKOVA DOMINIKA [1], BARTONICKOVA DANIELA [1,2], HOLUBOVA DOMINIKA [1], ZIAKOVA KATARINA [1]

[1] Department of Nursing, Jessenius Faculty of Medicine in Martin,
Comenius University in Bratislava, Slovak Republic
[2] Department of Nursing, Faculty of Health Sciences, Palacký University in Olomouc,
Czech Republic

Abstract

Introduction: The COVID-19 pandemic posed health and social threats and directly affected the quality and safe care. Many nursing students had mandatory practical training in hospitals to help the national system respond to the crisis. The investigation of nursing students´ perceptions of patient safety culture (PSC) might be beneficial in identifying safety areas that need improvement.

Aim: The pilot study aimed to investigate nursing students´ perception of PSC during the second wave of the COVID-19 pandemic.

Methods: The data were collected using the Hospital Survey on Patient Safety Culture - Nursing Students (HSOPS-NS). The HSOPS-NS tool was distributed online via the Google Forms platform between February and April 2021. The respondents studied in the 3rd year of the bachelor's degree in nursing (n = 66). Three nursing faculties from 3 regions in Slovakia were addressed. Descriptive statistics (mean, SD, frequency) was used for the sample characteristics and the HSOPS-NS tool. The Mann-Whitney U test and the Kruskal Wallis test analysed associations between sociodemographic data. The predictors of outcome dimensions of the HSOPS-NS were analysed by a multiple regression analysis.

Results: The nursing students evaluated the overall patient safety grade as very acceptable. Concerning PSC dimensions, the best-rated dimensions were "Feedback & communication about the error" (55.04%) and "Communication openness" (53.53%). The worst-rated dimensions were "Frequency of events reported" (33.32%) and "Staffing" (35.22%). A significant relationship was found between the perception of PSC and age, current area/unit, awareness of reporting systems, and supervision. The overall patient safety grade, the number of reported events, the number of reported events by nursing students were significantly predicted by several PSC dimensions (p ≤ 0.05).

Conclusions: The nursing students´ perspective on PSC revealed a weak perception of reporting adverse events. The awareness of reporting adverse events requires an increase in theoretical knowledge and the support of nursing students during their clinical training. A regular and comprehensive evaluation of PSC may strengthen patient safety and the overall awareness of patient safety among nursing students.

Keywords: Hospital Survey on Patient Safety Culture; nursing; student; patient safety culture

INTRODUCTION

Patient safety is a fundamental aspect leading to the depreciation of adverse events in healthcare systems. Interest in the issue is exponentially growing worldwide, mainly because it is a global problem that directly impacts patient care quality (1,2). The overall concept of

Corresponding author: Mgr. Dominika Kalánková, PhD.; e-mail: kalankova1@uniba.sk; Phone.: +421948 842 342; ORCID: 0000-0003-3396-3519

patient safety emerges from the Institute of Medicine (IOM) definition, referring to the "prevention of patient harm" (3). Providing patient safe care is a global challenge, and nurse education plays a pivotal role (4). In 1999, the IOM highlighted the need to include patient safety in the curricula of all healthcare professions. However, the extent to which this has been achieved is unknown and varies internationally (4,5). Initiatives focusing on these curricula have been developed in Europe, for example, by the European Federation of Nurses (EFN), the International Council of Nurses (ICN), the World Health Organization (WHO), and the European Network for Patient Safety (ENPS) (6). However, Tella et al. (7), based on their integrative literature review, revealed that patient safety in the nursing curriculum is still largely absent. They also recommended implementing specific methods related to patient safety in future nurses' theoretical and practical training. Furthermore, regular evaluation of this training is necessary (8). So far, there is no substantiated evidence of how nursing students understand and implement safety in clinical practice (9). At the same time, students´ experience from clinical practice may help identify threats to patient safety and increase students' knowledge and skills to improve it (8). One of the ways to increase their knowledge and skills can be to evaluate the PSC in the workplaces where their practice takes place. PSC is "a product of individual and group values, attitudes, perceptions, competencies and patterns of behaviour that determine an organization's relationship, style and expertise, as well as manage health and safety" (10). Assessing PSC can also be an essential element in ensuring patient safety in the future professional lives of nursing students (11). It has been shown that awareness of the patient safety context can influence, but also change, students' attitudes and behaviours towards the provision of quality and safe care (12). The evaluation of PSC is usually performed by various professional groups working in the hospital, e.g. managers, physicians, or nurses (13). Although students are a temporary but not yet fully qualified part of the nursing team, their views ("outside insights") on this issue have undeniable value not only for themselves but also for the management of healthcare facilities (1). Therefore, their perception of PSC should be regularly evaluated through an appropriate tool. For this pilot study, we attempted to investigate the nursing students´ perception of PSC during the second wave of the COVID-19 pandemic.

METHODS

The study adopted a cross-sectional design. The study was approved by the Ethics committee of the Jessenius Faculty of Medicine in Martin, Comenius University in Bratislava (EC no. 70/2020).

Sample

Three nursing faculties from three regions in the Slovak Republic were asked to participate in the pilot study. After being granted the permission by nursing faculties, the questionnaire was sent via email addresses by the nurse directors to the students in the 3rd year of the bachelor's degree in nursing. Altogether, at the time of the data collection, 194 nursing students were studying in the 3rd year. Due to the COVID-19 pandemic, the HSOPS-NS tool was distributed online via the Google Forms platform between February and April 2021.

Data collection

The data were collected using the Hospital Survey on Patient Safety Culture for Nursing Students (HSOPS-NS) questionnaire (1). The tool was designed to capture the nursing students´ perceptions of PSC. According to the authors of the original instrument, acceptable psychometric properties of the tool were confirmed in the validation study. As the tool was recommended as valid and reliable for evaluating nursing students´ perspectives of PSC, the Slovak version of the tool was created using the method of forward-backwards translation. The HSOPS-NS consists of 54 items grouped into four parts (A-D). Part A (Your workplace) includes 22 items and reflects the nursing students´ perceptions of a particular workplace

where they have clinical training. Part B (Your hospital) contains ten items through which students generally evaluate PSC in the hospital. Part C (Communication at the workplace) includes nine items and reflects nursing students' attitudes towards communication at the workplace where they have clinical training. The last part (D) contains eight items representing the additional information on the perception of PSC. The tool further includes five items capturing the overall perception of patient safety grade, the number of reported adverse events, the number of reported adverse events by the nursing students, the awareness of reporting systems, and additional notes about patient safety, errors, or reporting systems. These five items do not represent the core features of the HSOPS-NS. The students' responses are recorded using a 5-point Likert scale (strongly disagree to agree strongly). In additional items, the answers are recorded by a 10-point Likert scale or dichotomous options. Sociodemographic data in the tool include gender, age (up to 25 years; 26 years and more), the form of study (full-time students; part-time students), previous experiences with providing nursing care (have got experiences with care provision; have not got experiences with care provision), workplace (primary care; medical-surgical care units; intensive care units; mother-child inpatient care; other), and supervision during the clinical training (lecturer/teacher; nurse mentor with specific training in mentoring; nurse without specific training in mentoring).

Data analysis

The data were analysed in the statistical program IBM SPSS Statistics 25.0. The descriptive statistics (mean, SD, frequency) described the sample and the HSOPS-NS tool. The Mann-Whitney U test and the Kruskal Wallis test analysed associations between sociodemographic data. A multiple regression analysis was applied to determine the predictors of outcome dimensions of the HSOPS (Overall perceptions of patient safety, Number of events reported, Number of events reported by the nursing students). The results were tested on the significance level $p \leq 0.05$. The internal consistency based on Cronbach alpha coefficient (α) was 0.90 for the tool, indicating a very acceptable reliability.

RESULTS

The overall response rate was 34.02%. In the pilot study, 66 nursing students participated. Most of the respondents were females (92.5%), aged under 25 (75.7%; 27.15±9.81). More than half of the respondents were full-time students (66.7%) with previous experience with care provision (66.9%). Most of the nursing students (56.1%) were supervised by a nurse without any specific training in mentoring, followed by a nurse mentor with a specific training in mentoring (30.3%) and lecturer/teacher (13.6%). The nursing students worked primarily at medical-surgical care units (27.3%), followed by intensive care units (27.3%), primary care (18.2%), or other (18.2%) and mother-child inpatient care (10.6%).

Evaluation of the nursing students´ perceptions of PSC

The nursing students evaluated PSC dimensions under the expected level of 75% as recommended by the Agency for Healthcare Research and Quality (AHRQ) (15). The results are reported in detail in Table 1. The worst evaluated dimensions of PSC were "Frequency of events reported" (2.93 ± 0.97; 33.32%) and "Staffing" (3.02 ± 0.68; 35.22%). The best-evaluated dimensions of PSC were "Feedback & communication about error" (3.36 ± 1.07; 55.04%) and "Communication openness" (3.36 ± 0.91; 53.53%). On average, the nursing students evaluated the overall grade of patient safety as very good, with a mean value of 6.59. In addition, most of the nursing students (65.0%) were not aware of reporting any adverse events in the workplace they practised. The average number of reported events was 1.17 ± 2.17, ranging from 1 to 10. The nursing students' average number of reported events was 0.32 ± 0.76, ranging from 1 to 3. Besides, more than half of the nursing students (62.1%) were unaware of any adverse events reporting system.

Table 1 Dimensions of PSC

Safety culture dimensions	M ± SD	Positive responses
Teamwork within units	3.40 ± 0.87	52.27%
Supervisor/manager expectations & actions promoting patient safety	3.44 ± 0.86	53.02%
Organizational learning/continuous improvement	3.08 ± 0.92	37.87%
Management support for patient safety	3.31 ± 0.87	44.69%
Overall perceptions of patient safety	3.48 ± 0.73	53.38%
Feedback & communication about error	3.36 ± 1.07	55.04%
Communication openness	3.36 ± 0.91	53.53%
Frequency of events reported	2.93 ± 0.97	33.32%
Teamwork across units	3.23 ± 0.78	44.69%
Staffing	3.02 ± 0.68	35.22%
Handoffs & transitions	3.02 ± 0.37	38.63%
Nonpunitive responses to errors	3.26 ± 0.88	42.92%
Indicator of good praxis	3.28 ± 0.75	40.14%

Relationship between PSC dimensions and selected sociodemographic data

Mann-Whitney U test and Kruskal-Wallis test were used to test the relationship between the dimensions of PSC and selected sociodemographic data (the form of study, previous experience with care provision, age, the awareness of reporting systems, current unit or area, and supervision). The significant associations were not confirmed between the dimensions of PSC and the form of study and previous experience with care provision. In contrast, a significant relationship was proved between age and "Management support for patient safety", which was more positively reported by the nursing students aged less than 25 years (p=0.032). Similarly, the awareness of reporting systems was significantly associated with "Teamwork within units" and "Teamwork across units", which were better evaluated by the nursing students aware of the reporting systems (p=0.020 respectively p=0.048). A significant relationship was proved between the current unit or area and several dimensions of PSC. "Teamwork within units" (p=0.001) and "Overall perceptions of patient safety" (p=0.017) were significantly better evaluated by the students practising at intensive care units. In contrast, "Supervisor/manager expectations & actions promoting patient safety" (p=0.049) and "Nonpunitive responses to errors" (p=0.048) were significantly better perceived by the students practising in primary care settings. Moreover, significant associations were confirmed between supervision and the "Frequency of events reported" (p=0.007), which was better evaluated by the students supervised during their practice by a lecturer/teacher (an employee of the nursing faculty).

Results from multiple regression analysis

A multiple regression analysis was conducted to examine the relationship between the overall grade of patient safety, the number of reported events in the workplace, the number of reported events by the nursing students, and the dimensions of PSC. The results are presented in Table 2. Model 1 (R^2=0.414; Adj R^2=0.268; F=2.832; p=0.004) revealed the overall

grade of patient safety was significantly associated with the following dimensions – "Management support for patient safety" (β= 0.317; p=0.029) and "Overall perceptions of patient safety" (= 0.444; p=0.010). The nursing students who better evaluated the overall patient safety grade also perceived "Management support for patient safety" more positively and reported better "Overall perceptions of patient safety". Model 2 (R^2=0.352; Adj R^2=0.184; F=2.090; p=0.032) confirmed a significant relationship between the number of reported events and the following dimensions – "Overall perceptions of patient safety" (β = -0.655; p=0.001) and "Handoffs & transitions" (β= -0.246; p=0.046). A higher number of events was reported in the workplace which the nursing students evaluated in terms of "Overall perceptions of patient safety" as worse. Similarly, a higher number of events was reported in the workplace which the nursing students evaluated in terms of "Handoffs & transitions" as worse. In Model 3 (R^2= 0.295; Adj R^2=0.118; F=1.671; p=0.006) revealed a significant relationships between the number of reported events by the nursing students and the following dimensions of PSC – "Teamwork within units" (β= -0.482; p=0.006), "Overall perceptions of patient safety" (β= -0.435; p=0.021), and "Handoffs & transitions" (β= -0.208; p=0.039). A higher number of events was reported by the nursing students who evaluated the dimensions mentioned above of patient safety as worse.

Table 2 Outcome dimensions and their relationship to dimensions of PSC

Dimensions of PSC **	Overall grade of patient safety		Number of events reported		Number of events reported by the nursing students	
	β coefficient*	p-value	β coefficient	p-value	β coefficient	p-value
D1	-0.059	0.704	0.067	0.688	-0.482	**0.006**
D2	-0.091	0.630	0.308	0.133	0.188	0.365
D3	-0.227	0.190	-0.027	0.886	0.082	0.666
D4	0.317	**0.029**	-0.176	0.254	-0.015	0.921
D5	0.444	**0.010**	-0.655	**0.001**	-0.435	**0.021**
D6	0.319	0.111	-0.044	0.838	-0.124	0.570
D7	-0.185	0.246	0.188	0.271	0.173	0.324
D8	0.136	0.403	0.085	0.634	0.244	0.174
D9	0.075	0.627	0.203	0.235	-0.190	0.267
D10	-0.023	0.860	0.218	0.138	0.049	0.733
D11	-0.043	0.734	-0.246	**0.046**	-0.208	**0.039**
D12	-0.171	0.252	-0.122	0.449	0.168	0.305
D13	0.049	0.773	0.104	0.568	-0.243	0.193

*Standardized β coefficient; **D1 - Teamwork within units; D2 - Supervisor/manager expectations & actions promoting patient safety; D3 - Organizational learning/continuous improvement; D4 - Management support for patient safety; D5 - Overall perceptions of patient safety; D6 - Feedback & communication about error; D7 - Communication openness; D8 - Frequency of events reported; D9 - Teamwork across units; D10 – Staffing; D11 - Handoffs & transitions; D12 - Nonpunitive responses to errors; D13 – Indicator of good praxis

DISCUSSION

The pilot study aimed to investigate the nursing students´ perception of PSC during the second wave of the COVID-19 pandemic. Recent studies (6, 8) have shown that nursing students might bring a broader perspective to the issue of PSC. Nursing students´ perceptions of PSC are essential to identify the strengths and weaknesses of care provision but also the safety issues in their education that need to be improved. It has been reported that approximately 80% of students acquired information about patient safety during their clinical practice. These students then perceived patient safety more positively (14). The results of our pilot study showed that the nursing students evaluated PSC under the expected level of 75% as recommended by AHRQ in all dimensions (15). The worst evaluated dimensions of PSC were "Staffing" and "Frequency of events" reported. Nurse shortage has been proven to significantly impact response to patient safety agenda, including reporting practices of Slovak nurses (16). However, the issue of nurse shortage remains a global problem, often resulting in underreporting of adverse events (17, 18). In contrast, the best-evaluated dimension of PSC, but still under the expectance level, was "Feedback & communication about error", involving "Communication openness". The Slovak nurses reported similar results. The results of the study suggest that nursing perceptions on the dimensions of PSC are very similar to those reported by the Slovak nurses (19, 20). This might be due to their lack of awareness of patient safety and, at the same time, to the fact that the subject of patient safety has only recently been included in their curricula at some faculties in Slovakia. Still, there are inconsistencies in patient safety teaching across nursing faculties that might lead to weak perceptions of PSC among students. The nursing students´ perception of PSC was captured in two studies worldwide. In a study by Kong et al. (14), a positive response for all six evaluated domains was below 55%, with "Stress recognition" being the best rated and "Safety climate" the worst. In a study by Çiftcioğlu et al. (21), the safety score was found to be moderate, and the students rated "Care environment" and "Employee behaviour" the best and "Training of employees" the worst. However, it should be noted that in both studies other instruments were used to assess the perception of nursing students and their perception was not, as with nurses from Slovak studies (19,20), marked by the COVID-19 pandemic.

Interestingly, during the second wave of COVID-19, the nursing students evaluated the overall grade of patient safety quite positive (6.59; 65.9 %), which is comparable to the nurses from Slovakia. They, however, evaluated through the HSOPS the overall grade of patient safety instead of 10, the highest value of 5 (in percentages: 72.6%). It was surprising that more than half of the students had no awareness of events reporting on the workplaces where they practised. Often the students are not involved in these matters, although it is very important to train them sufficiently about reporting errors. In addition, they should know that if an adverse event occurs, it is better to report it before it causes an injury. At the same time, non-repressive environments should be encouraged and promoted, where healthcare workers do not have to be afraid to report an adverse event because they will not be punished (15). In connection with the unconsciousness, but perhaps also the lack of time of the nurses, the students who gained awareness of the reporting of adverse events during the clinical practice knew only about two events reported by the nurses and by them alone, a maximum of 0.76 were reported on average.

If we consider the factors influencing the nursing students' perception regarding PSC dimensions, then in our study "Teamwork within units" and "Teamwork across units" were better rated by the nursing students aware of the reporting systems. In addition, "Teamwork across units" was also ponderable by the students practising at intensive care units. These students also better evaluated the "Overall perceptions of patient safety". Regarding "Management support for patient safety", it was better appraised by the students aged under 25 and "Supervisor/ manager expectations & actions promoting patient safety" and "Nonpunitive responses to errors" were better perceived by the students practising in pri-

mary care settings. The last but not least significant relationship was that if the students were supervised during their practice by a lecturer/teacher, they marked better the "Frequency of events reported". This may be a way to make them more aware. However, the internship in Slovakia does not explicitly occur under a lecturers´ guidance, whereas their presence in the internship is irreplaceable and very well evaluated by the students (22).

Regarding the relationship between the overall grade of patient safety, the number of reported events in the workplace, and the dimensions of PSC, statistically significant relationships were also demonstrated as in the case of nurses, e.g. in the Czech Republic (23) or Slovakia (16,20). In addition, a higher incidence of the number of reported events by the nursing students associated with a worse assessment of "Teamwork within units", "Overall perceptions of patient safety", and "Handoffs & transitions" was demonstrated in our study, which has not been investigated in any other studies. The better-evaluated dimension "Overall grade of patient safety" by the students in our study was significantly associated with more positively perceived "Management support for patient safety" and "Overall perceptions of patient safety". In a study by Bartoníčková et al. (23) and Gurková et al. (20), the "Overall perception of patient safety" as an independent variable was significantly associated with, for example, a positive perception of "Staffing", "Organizational learning and continuous improvement", "Supervisor/manager expectations & actions promoting patient safety" but also "Management support for patient safety". A higher number of events reported by the students in our study connected with worse evaluated "Overall perception of patient safety" and "Handoffs & transitions". In a study by Bartoníčková et al. (23), higher ratings in the frequency of events reported by nurses were connected with positive "Feedback and communication about error", "Organizational learning, and continuous improvement".

To the authors´ knowledge, there is no international study focusing on nursing students´ perspectives on PSC during their practice and, at the same time, during the COVID-19 pandemic through the HSOPS-NS instrument. Several studies recently focused on nursing students´ perception of COVID-19 and coping with stress, while most of them indicated that students perceived moderate levels of stress and anxiety during the COVID-19 pandemic (24-26). However, it is a question because the integration of students into practice during the COVID-19 pandemic took place very differently internationally.

The study has several limitations. The first limitation is the inclusion of a non-randomized sample of nursing students and the integration of only three nursing faculties from Slovakia. Larger sample size will also enable testing the psychometric properties of the HSOPS-NS instrument. Based on the pilot study results, we aim to conduct a further study with a larger sample size and more nursing faculties included. Another limitation is the administration of self-reported measures so that social desirability might influence results.

CONCLUSION

During the mandatory practical training, the students who are part of the nursing team can significantly complement the assessment of the construct of PSC perceived by the nurses and, thus, impartially reflect the multidimensional aspects that determine the provision of safe care. In Slovakia, the nursing students' overall perception of patient safety was positively rated. The best-rated dimensions were those related to communication and the worst-rated were the staffing and frequency of events reported. It is evident that the nursing students' reporting of adverse events in Slovakia is outlawed. However, in terms of factors, the presence of lecturers or teachers during the internships could contribute to their improvement. The medical workplace management can use this benefit to increase the quality of care. It can also positively affect strengthening knowledge and positive attitudes towards PSC in the undergraduate training of future nurses.

REFERENCES

1. De Elguea JO, Orkaizagirre-Gómaa A, De Miguel MS, Urcola-Pardo F, Germán-Bes C, Lizaso-Elgaresta. Adapting and validating the Hospital Survey on Patient Safety Culture (HSOPS) for nursing students (HSOPS-NS): A new measure of Patient Safety Climate. Nurse Educ Today 2019; 75:95-103.
2. Pousette A, Larsman P, Eklöf M, Törner M. The relationship between patient safety climate and occupational safety climate in healthcare – A multi-level investigation. J Safety Res 2017; 61: 187-198.
3. Institute of Medicine. Keeping patients safe: transforming the work environment of nurses. Washington (DC): National Academies Press; 2004.
4. Steven A, Magnusson C, Smith P, Pearson PH. Patient safety in nursing education: contexts, tensions and feeling safe to learn. Nurse Educ Today 2014; 34(2):277-84.
5. Kohn LT, Corrigan JM, Donaldson MS, eds. To err is human: building a safer health system. Washington, DC: National Academy Press; 1999.
6. Kirwan M, Riklikiene O, Gotlib J, Fuster P, Borta M. Regulation and current status of patient safety content in pre-registration nurse education in 27 countries: Findings from the rationing – Missed nursing care (RANCARE) project. Nurse Educ Pract 2019; 37: 132-140.
7. Tella S, Smith NJ, Partanen P. Learning to ensure patient safety in clinical settings: comparing Finnish and British nursing students' perceptions. J Clin Nurs 2015; 24(19-20): 2954-2964.
8. Mansour MJ, Al Shadafan SF, Abu-Sneineh FT, AlAmer MM. Integrating Patient Safety Education in the Undergraduate Nursing Curriculum: A Discussion Paper. Open Nurs J 2018; 12: 125-132.
9. Mansour M. Current assessment of patient safety education. Br J Nurs 2012; 21(9): 536-543.
10. Sorra JS, Nieva VF. Hospital Survey on Patient Safety Culture [online]. 2004 [cited 2021 Feb 03]. Available from: https://www.ahrq.gov/
11. Palese A, Gonella S, Grassetti L, Mansutti I, Brugnolli A, Saiani L, Terzoni S, Zannini L, Destrebecq A, Dimonte V. Multi-level analysis of national nursing students' disclosure of patient safety concerns. Med Educ 2018; 52(11): 1156-1166.
12. Liao JM, Etchegaray JM, Williams ST, Berger DH, Bell SK, Thomas EJ. Assessing medical students' perceptions of patient safety: the medical student safety attitudes and professionalism survey. Acad Med 2014; 89(2): 343–351.
13. Singer SJ, Falwell A, Gaba DM, Meterko M, Rosen A, Hartmann CW, Baker L. Identifying organizational cultures that promote patient safety. Health Care Manage Rev 2009; 34(4): 300-311.
14. Kong L-N, Zhu W-F, He S, Chen S-Z, Yang L, Qi L, Peng X. Attitudes towards patient safety culture among postgraduate nursing students in China: A cross-sectional study. Nurse Educ Pract 2019; 38: 1-6.
15. Ammouri AA, Tailakh AK, Mullira JK, Geethakrishnan R, Al Kindi SN. Patient safety culture among nurses. Int Nurs Rev 2015;62(1): 102-110.
16. Kalánková D, Kirwan M, Bartoníčková D, Kurucová R, Žiaková K, Gurková E. How adverse event reporting in the Slovak Republic is influenced by nurse characteristics and working arrangements: a cross-sectional study. KONTAKT 2021; 23(2): 97-103.
17. McLennan SR, Diebold M, Rich LE, Elger BS. Nurses' perspectives regarding the disclosure of errors to patients: A qualitative study. Int J Nurs Stud 2016; 54: 16–22.
18. Prang IW, Jelsness-Jørgensen L-P. Should I report? A qualitative study of barriers to incident reporting among nurses working in nursing home. Geriatr Nurs 2014; 35(6): 441–447.
19. Kalánková D, Bartoníčková D, Žiaková K, Gurková E, Kurucová R. Assessment of the safety climate at university hospitals in the Slovak Republic from the nurses´ perspective. Acta Med Martiniana 2020; 20(1): 27-38.
20. Gurková E, Kalánková D, Kurucová R, Žiaková K. Assessment of patient safety climate by nurses in Slovak public and private hospitals. J Nurs Manag 2020; 28(7): 1644-1655.
21. Çiftcioğlu Ş, Cırık VA, Efe E. Student nurses´ perceptions of a patient safety culture: A descriptive and cross-sectional study [published online ahead of print, 2021 Apr 30]. Perspect Psychiatr Care 2021. https://doi.org/10.1111/ppc.12830

22. Mikkonen K, Tomietto M, Tuomikoski A-M, Miha Kaučič B, Riklikiene O, Vizcaya Moreno F, Pérez Cañaveras RM, Filej B, Baltinaite G, Cicolini G, Kääriäinen M. Mentors' competence in mentoring nursing students in clinical practice: Detecting profiles to enhance mentoring practices. Nurs Open 2022; 9(1): 593-603.
23. Bartoníčková D, Kalánková D, Mikšová Z, Žiaková K, Mazalová L. Patient safety culture from a nursing point of view in a broader context. KONTAKT 2019; 21(2):121-127.
24. Akay G, Kadiroglu T. Covid-19 Perception of Senior Nursing Students and their Behaviours Regarding Coping with Stress. Int Arch Nurs Health Care 2021; 7:161.
25. Aslan H, Pekince H. Nursing students' views on the COVID-19 pandemic and their percieved stress levels. Perspect Psychiatr Care 2021;57(2): 695-701.
26. Hernández-Martínez A, Rodríguez-Almagro J, Martínez-Arce A, Romero-Blanco C, García-Iglesias JJ, Gómez-Salgado J. Nursing students' experience and training in healthcare aid during the COVID-19 pandemic in Spain [published online ahead of print, 2021 Feb 15]. J Clin Nurs 2021. https://doi.org/10.1111/jocn.15706